

CEvNS as a tool to investigate nuclear and electroweak properties: current status and prospects

Magnificent CEvNS 2023 22-29 Mar 2023



Matteo Cadeddu
matteo.cadeddu@ca.infn.it



In collaboration with

M. Atzori Corona
N. Cargioli
F. Dordei
C. Giunti
G. Masia
Y. F. Li
C. A. Ternes
Y. Y. Zhang

Coherent elastic neutrino nucleus scattering (aka CEνNS)

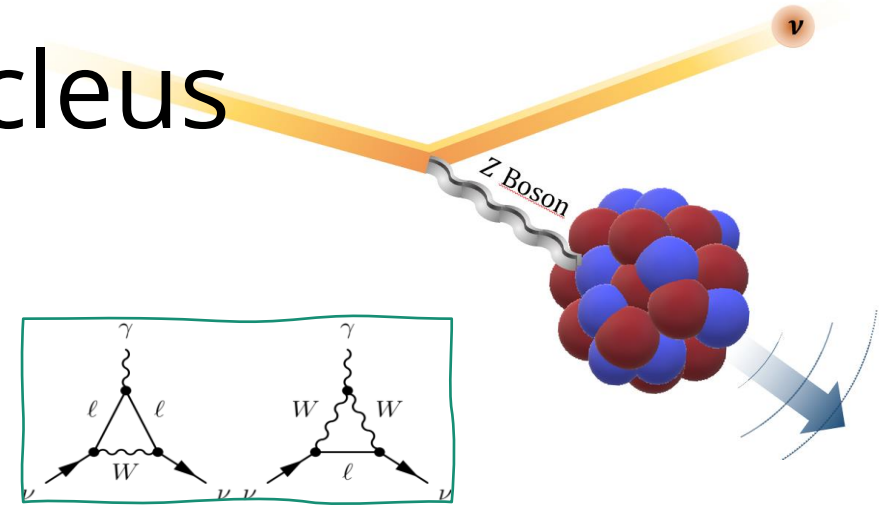
+ A pure weak neutral current process

$$\frac{d\sigma_{\nu\ell-\mathcal{N}}}{dT_{\text{nr}}}(E, T_{\text{nr}}) = \frac{G_F^2 M}{\pi} \left(1 - \frac{MT_{\text{nr}}}{2E^2}\right) (Q_{\ell, \text{SM}}^V)^2$$

+ Weak charge of the nucleus

$$Q_{\ell, \text{SM}}^V = \underbrace{[g_V^p(\nu_\ell) Z F_Z(|\vec{q}|^2)]}_{\text{protons}} + \underbrace{g_V^n N F_N(|\vec{q}|^2)}_{\text{neutrons}}$$

In general, in a weak neutral current process which involves nuclei, one deals with **nuclear form factors** that are different for **protons** and **neutrons** and cannot be disentangled from the neutrino-nucleon couplings!



+ Neutrino-nucleon **tree-level** couplings

$$g_V^p = \frac{1}{2} - 2 \sin^2(\vartheta_W) \approx 0.02274$$

$$g_V^n = -\frac{1}{2} = -0.5$$

J. Erler and S. Su. *Prog. Part. Nucl. Phys.* 71 (2013). arXiv:1303.5522 & PDG2022

+ Radiative corrections are expressed in terms of WW, ZZ boxes and the **neutrino charge radius** diagram → **Flavour dependence**

$$g_V^p(\nu_e) = 0.0382, g_V^p(\nu_\mu) = 0.0300 \text{ and } g_V^n = -0.5117$$

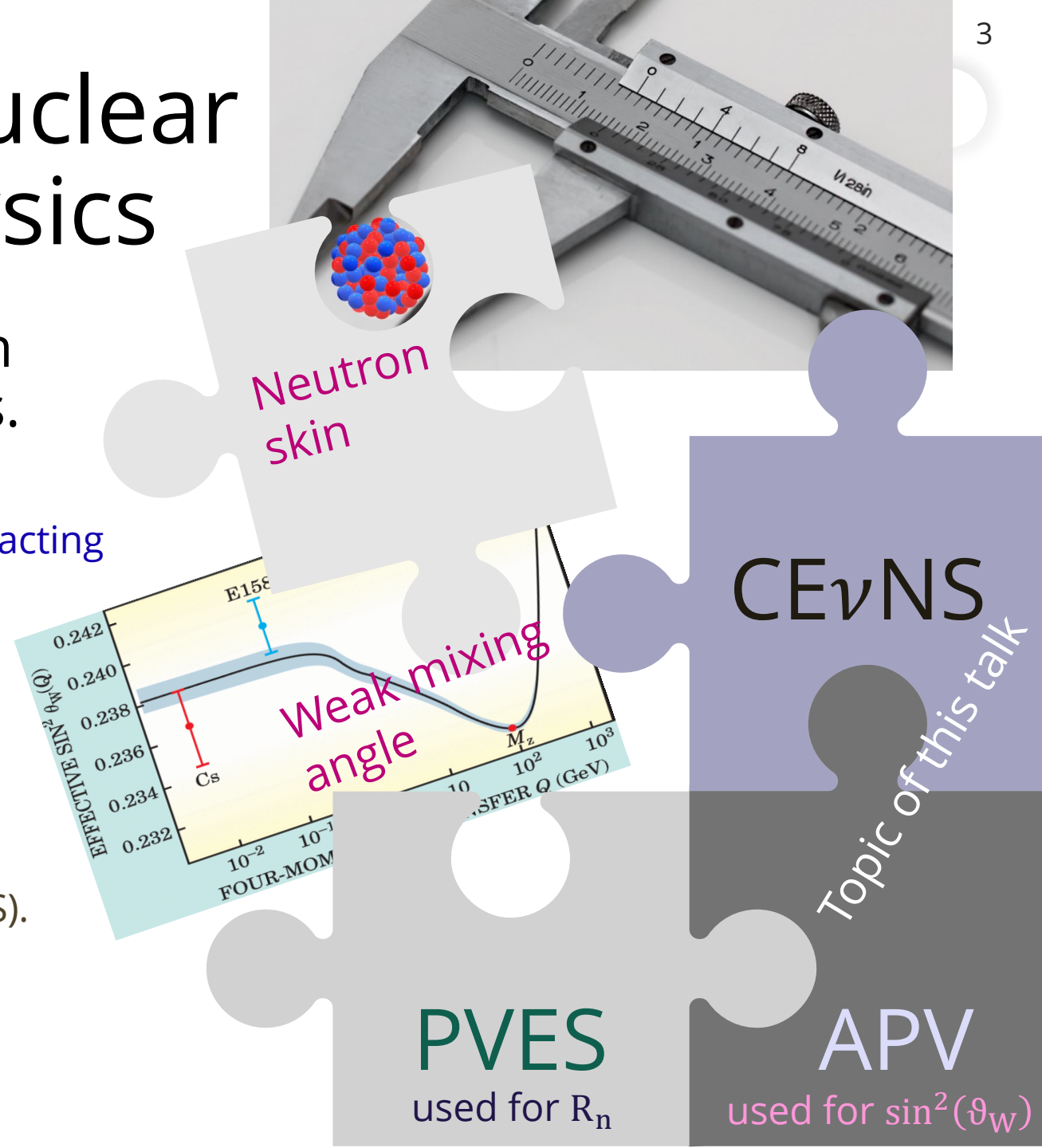
Nuclear physics, but since $g_V^n \approx -0.51 \gg g_V^p(\nu_\ell) \approx 0.03$ neutrons contribute the most

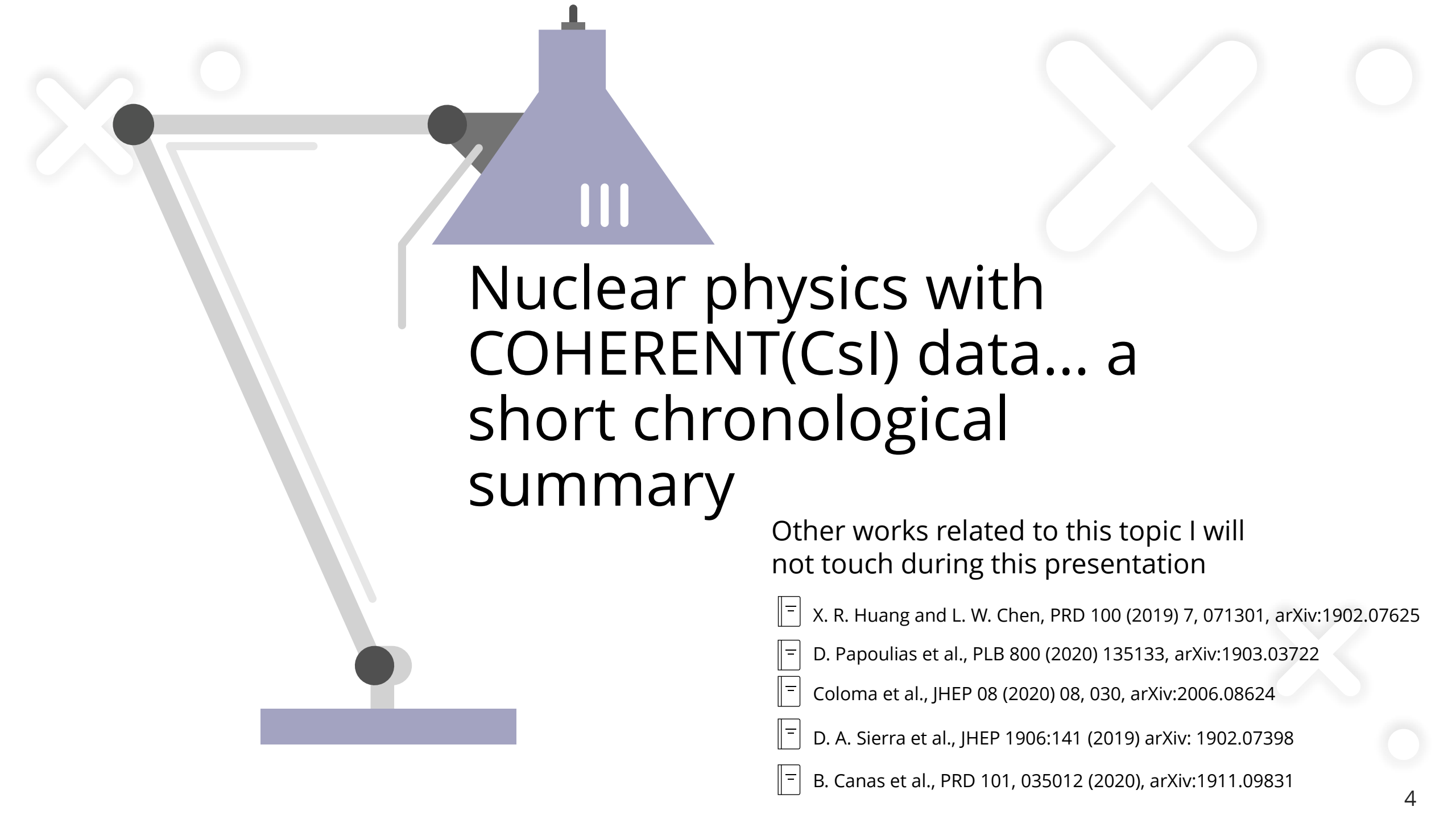
$$\frac{d\sigma}{dE_r} \propto N^2$$

Interplay between nuclear and electroweak physics

+ This feature is always present when dealing with electroweak processes.

- Atomic Parity Violation (APV): atomic electrons interacting with nuclei. Cesium available.
- Parity Violation Electron Scattering (PVES): polarized electron scattering on nuclei. PREX(Pb), CREX(Ca)
- Coherent elastic neutrino-nucleus scattering (CE ν NS). Cesium-iodide (CsI), argon (Ar) and germanium (Ge) available.





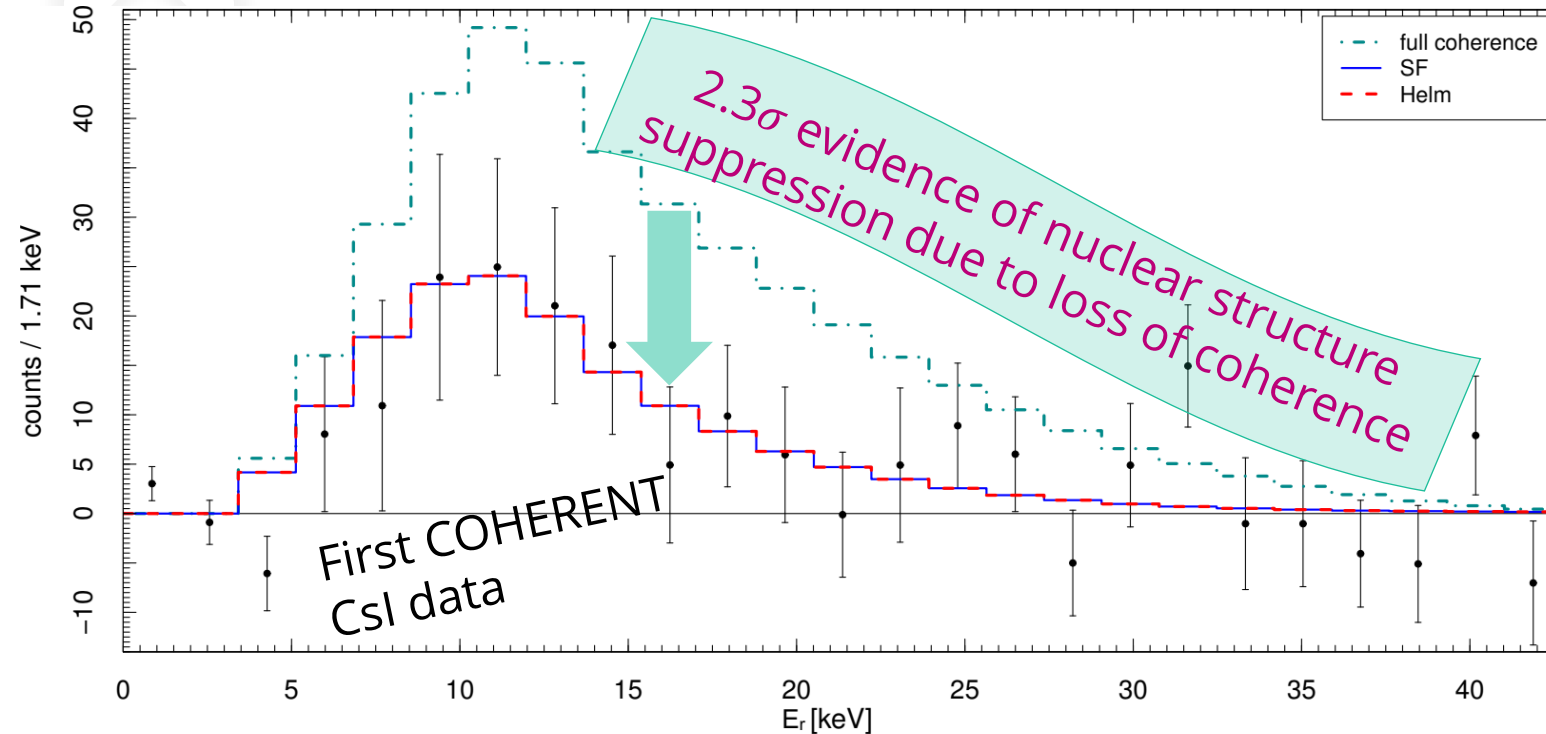
Nuclear physics with COHERENT(CsI) data... a short chronological summary


Other works related to this topic I will
not touch during this presentation

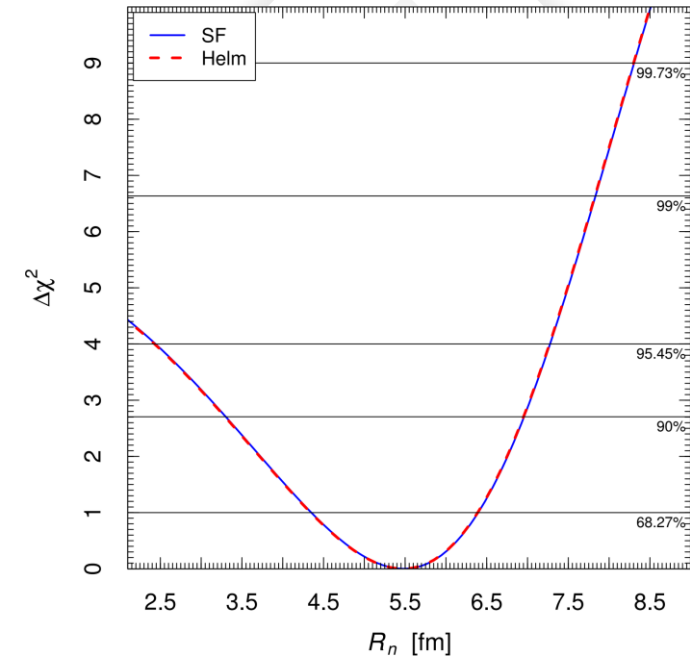
- [-] X. R. Huang and L. W. Chen, PRD 100 (2019) 7, 071301, arXiv:1902.07625
- [-] D. Papoulias et al., PLB 800 (2020) 135133, arXiv:1903.03722
- [-] Coloma et al., JHEP 08 (2020) 08, 030, arXiv:2006.08624
- [-] D. A. Sierra et al., JHEP 1906:141 (2019) arXiv: 1902.07398
- [-] B. Canas et al., PRD 101, 035012 (2020), arXiv:1911.09831

First average Csl neutron radius measurement (2018)

+ Using the first Csl dataset from  D. Akimov et al. **Science** 357.6356 (2017)



 M. Cadeddu, C. Giunti, Y.F. Li, Y.Y. Zhang, PRL 120 072501, (2018), arXiv:1710.02730



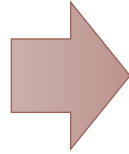
$$R_n^{\text{Csl}} = 5.5_{-1.1}^{+0.9} \text{ fm}$$

- We first compared the data with the predictions in the case of full coherence, i.e. all nuclear form factors equal to unity: the corresponding histogram does not fit the data.
- We fitted the COHERENT data in order to get information on the value of the neutron rms radius R_n , which is determined by the minimization of the χ^2 using the symmetrized Fermi ($t=2.3$ fm) and Helm form factors ($s=0.9$ fm).

- ✓ Only energy information used
- ✗ No energy resolution
- ✗ No time information
- ✗ Small dataset and big syst. uncer.

The Csl neutron skin (in 2018)

$$R_n^{CsI} = 5.5_{-1.1}^{+0.9} \text{ fm}$$



Proton rms radius for Cs and I

$$R_p^{Cs} = 4.821(5) \text{ fm and}$$

$$R_p^I = 4.766(8) \text{ fm}$$

are around 4.78 fm, with a difference of about 0.05 fm

The neutron skin

$$\Delta R_{np}^{CsI} \equiv R_n - R_p \cong 0.7_{-1.1}^{+0.9} \text{ fm}$$

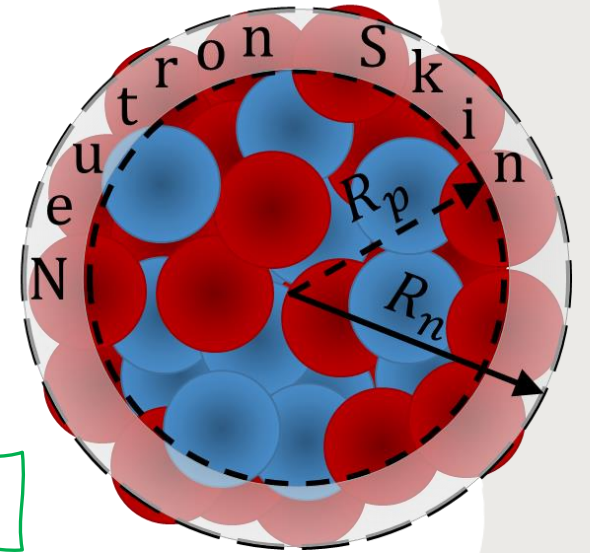
[=] G. Fricke et al., At. Data Nucl. Data Tables **60**, 177 (1995).

Theoretical values of the proton and neutron rms radii of Cs and I obtained with nuclear mean field models. The value was compatible with all the models...

Model	¹²⁷ I						¹³³ Cs					
	R_p^{point}	R_p	R_n^{point}	R_n	$\Delta R_{np}^{\text{point}}$	ΔR_{np}	R_p^{point}	R_p	R_n^{point}	R_n	$\Delta R_{np}^{\text{point}}$	ΔR_{np}
SHF SkI3 [81]	4.68	4.75	4.85	4.92	0.17	0.17	4.74	4.81	4.91	4.98	0.18	0.18
SHF SkI4 [81]	4.67	4.74	4.81	4.88	0.14	0.14	4.73	4.80	4.88	4.95	0.15	0.14
SHF Sly4 [82]	4.71	4.78	4.84	4.91	0.13	0.13	4.78	4.85	4.90	4.98	0.13	0.13
SHF Sly5 [82]	4.70	4.77	4.83	4.90	0.13	0.13	4.77	4.84	4.90	4.97	0.13	0.13
SHF Sly6 [82]	4.70	4.77	4.83	4.90	0.13	0.13	4.77	4.84	4.89	4.97	0.13	0.13
SHF Sly4d [83]	4.71	4.79	4.84	4.91	0.13	0.12	4.78	4.85	4.90	4.97	0.12	0.12
SHF SV-bas [84]	4.68	4.76	4.80	4.88	0.12	0.12	4.74	4.82	4.87	4.94	0.13	0.12
SHF UNEDF0 [85]	4.69	4.76	4.83	4.91	0.14	0.14	4.76	4.83	4.92	4.99	0.16	0.15
SHF UNEDF1 [86]	4.68	4.76	4.83	4.91	0.15	0.15	4.76	4.83	4.90	4.98	0.15	0.15
SHF SkM* [87]	4.71	4.78	4.84	4.91	0.13	0.13	4.76	4.84	4.90	4.97	0.13	0.13
SHF SkP [88]	4.72	4.80	4.84	4.91	0.12	0.12	4.79	4.86	4.91	4.98	0.12	0.12
RMF DD-ME2 [89]	4.67	4.75	4.82	4.89	0.15	0.15	4.74	4.81	4.89	4.96	0.15	0.15
RMF DD-PC1 [90]	4.68	4.75	4.83	4.90	0.15	0.15	4.74	4.82	4.90	4.97	0.16	0.15
RMF NL1 [91]	4.70	4.78	4.94	5.01	0.23	0.23	4.76	4.84	5.01	5.08	0.25	0.24
RMF NL3 [92]	4.69	4.77	4.89	4.96	0.20	0.19	4.75	4.82	4.95	5.03	0.21	0.20
RMF NL-Z2 [93]	4.73	4.80	4.94	5.01	0.21	0.21	4.79	4.86	5.01	5.08	0.22	0.22
RMF NL-SH [94]	4.68	4.75	4.86	4.94	0.19	0.18	4.74	4.81	4.93	5.00	0.19	0.19

Theoretically

$$0.12 < \Delta R_{np}^{CsI} < 0.24 \text{ fm}$$



But this is not the end of the story...
In 2020 the COHERENT
Collaboration released the full Csl
dataset



Improvements with the latest CsI dataset

+ New quenching factor

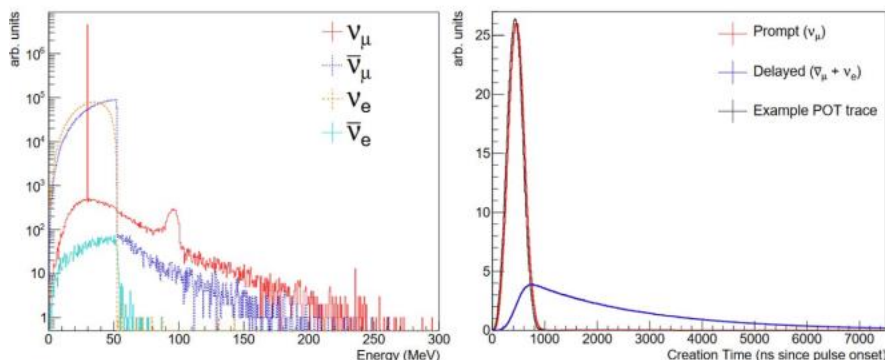
$$E_{ee} = f(E_{nr}) = aE_{nr} + bE_{nr}^2 + cE_{nr}^3 + dE_{nr}^4.$$

$$a=0.05546, b=4.307, c=-111.7, d=840.4$$

[-] Akimov et al. (COHERENT Coll), arXiv:2111.02477, JINST 17 P10034 (2022)

+ 2D fit, arrival time information included

$$N_{ij}^{\text{CE}\nu\text{NS}} = (N_i^{\text{CE}\nu\text{NS}})_{\nu_\mu} P_j^{(\nu_\mu)} + (N_i^{\text{CE}\nu\text{NS}})_{\nu_e, \bar{\nu}_\mu} P_j^{(\nu_e, \bar{\nu}_\mu)}$$



+ Doubled the statistics and reduced syst. uncertainties

$$\sigma_{\text{CE}\nu\text{NS}} = 13\%, \sigma_{\text{BRN}} = 0.9\%,$$

$$\text{and } \sigma_{\text{SS}} = 3\%$$

➤ Theoretical number of CE ν NS events

$$N_i^{\text{CE}\nu\text{NS}} = N(\text{CsI}) \int_{T_{\text{nr}}^i}^{T_{\text{nr}}^{i+1}} dT_{\text{nr}} A(T_{\text{nr}}) \int_0^{T_{\text{nr}}^{\text{max}}} dT'_{\text{nr}} R(T_{\text{nr}}, T'_{\text{nr}}) \int_{E_{\text{min}}(T'_{\text{nr}})}^{E_{\text{max}}} dE$$

$$\times \sum_{\nu=\nu_e, \nu_\mu, \bar{\nu}_\mu} \frac{dN_\nu}{dE}(E) \frac{d\sigma_{\nu\text{-CsI}}}{dT'_{\text{nr}}}(E, T'_{\text{nr}}),$$

➤ With the inclusion of energy resolution

$$R(N_{\text{PE}}, N'_{\text{PE}}) = \frac{[a_R(1+b_R)]^{1+b_R}}{\Gamma(1+b_R)} N_{\text{PE}}^{b_R} e^{-a_R(1+b_R)N_{\text{PE}}}$$

✓ Analysis with a Gaussian least-square function

$$\chi_C^2 = \sum_{i=2}^9 \sum_{j=1}^{11} \left(\frac{N_{ij}^{\text{exp}} - \sum_{z=1}^3 (1 + \eta_z) N_{ij}^z}{\sigma_{ij}} \right)^2 + \sum_{z=1}^3 \left(\frac{\eta_z}{\sigma_z} \right)^2,$$

[-] Cadeddu et al., PRC 104, 065502 (2021), arXiv:2102.06153



Analysis updated in this talk using a Poissonian least-square function after the COHERENT data release!

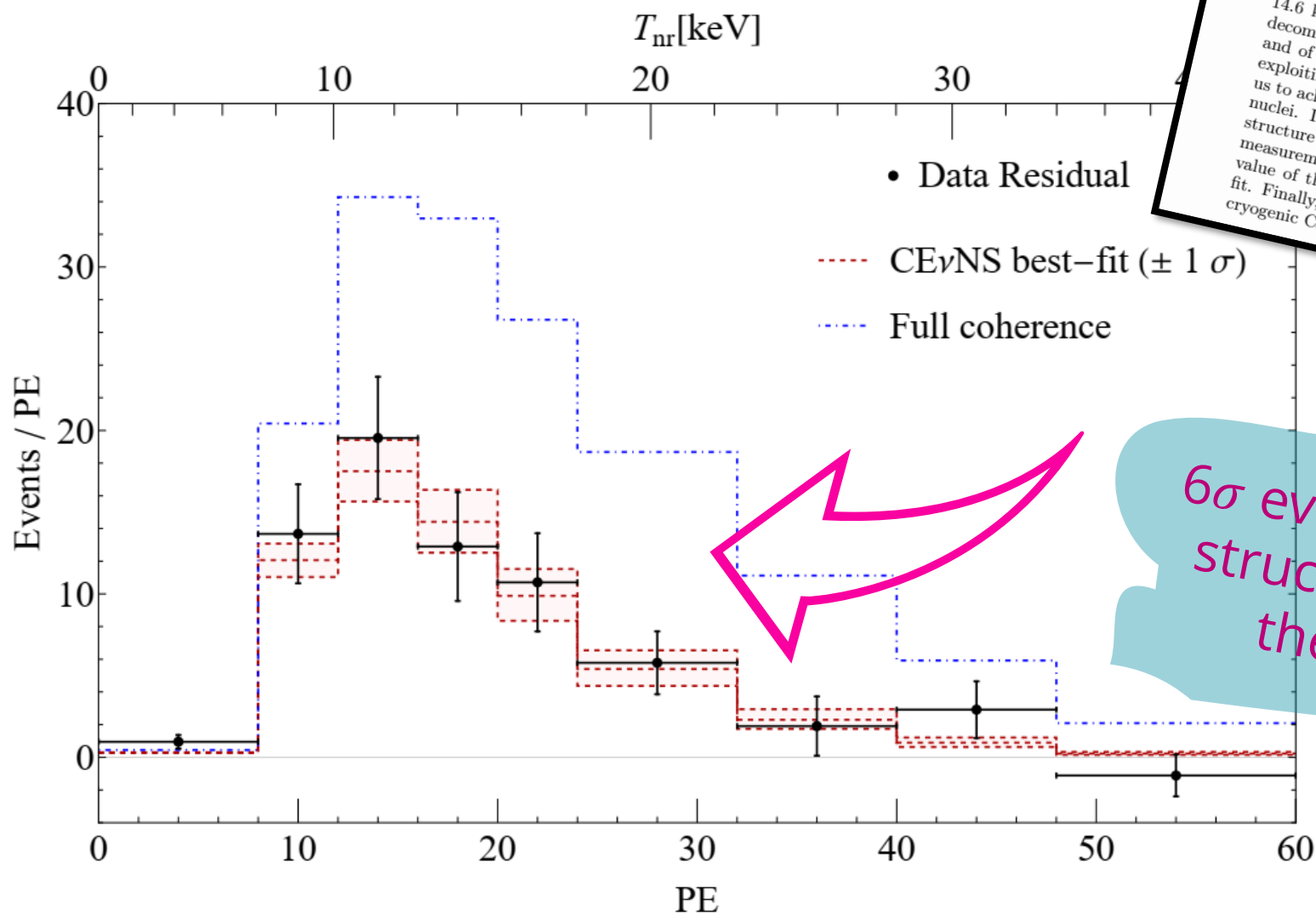


It appeared last week on [arXiv:2303.09360](https://arxiv.org/abs/2303.09360)



Suppression of the full coherence

$$\frac{d\sigma_{\nu\ell-N}}{dT_{\text{nr}}}(E, T_{\text{nr}}) = \frac{G_F^2 M}{\pi} \left(1 - \frac{MT_{\text{nr}}}{2E^2}\right) [g_V^p(\nu_\ell) Z F_Z(|\vec{q}|^2) + g_V^n N F_N(|\vec{q}|^2)]^2$$



Nuclear neutron radius and weak mixing angle measurements from latest COHERENT CsI and atomic parity violation Cs data

M. Atzori Corona,^{1,2,*} M. Cadeddu,^{2,*} N. Cargioli,^{1,2,*} F. Dordei,^{2,*} C. Giunti,^{3,*} and G. Masia^{1,**}

¹Dipartimento di Fisica, Università degli Studi di Cagliari, Complesso Universitario di Monserrato - S.P. per Sestu Km 0.700, 09042 Monserrato (Cagliari), Italy

²Istituto Nazionale di Fisica Nucleare (INFN), Sezione di Cagliari, Complesso Universitario di Monserrato - S.P. per Sestu Km 0.700, 09042 Monserrato (Cagliari), Italy

³Istituto Nazionale di Fisica Nucleare (INFN), Sezione di Torino, Via P. Giuria 1, I-10125 Torino, Italy

(Dated: Friday 17/03/23, 00:39)

The COHERENT collaboration observed coherent elastic neutrino nucleus scattering using a 14.6 kg cesium-iodide (CsI) detector in 2017 and recently published the updated results before decommissioning the detector. Here, we present the legacy determination of the weak mixing angle and of the average neutron rms radius of ^{133}Cs and ^{127}I obtained with the full CsI dataset, also exploiting the combination with the atomic parity violation (APV) experimental result, that allows us to achieve a precision as low as $\sim 4.5\%$ and to disentangle the contributions of the ^{133}Cs and ^{127}I nuclei. Interestingly, we show that the COHERENT CsI data show a 6σ evidence of the nuclear structure suppression of the low-energy weak mixing angle. Moreover, we derive a data-driven APV+COHERENT measurement of the average neutron rms radius of ^{133}Cs and ^{127}I , that is allowed to vary freely in the fit. Finally, in light of the recent announcement of a future deployment of a 10 kg and a ~ 700 kg cryogenic CsI detectors, we provide future prospects for these measurements.

6σ evidence of the nuclear structure suppression of the full coherence!

The CsI neutron skin (2023 update)

M. Atzori Corona et al., arXiv:2303.09360

$$R_n(\text{CsI}) = 5.47 \pm 0.38 \text{ fm}$$

Average proton rms radius for CsI

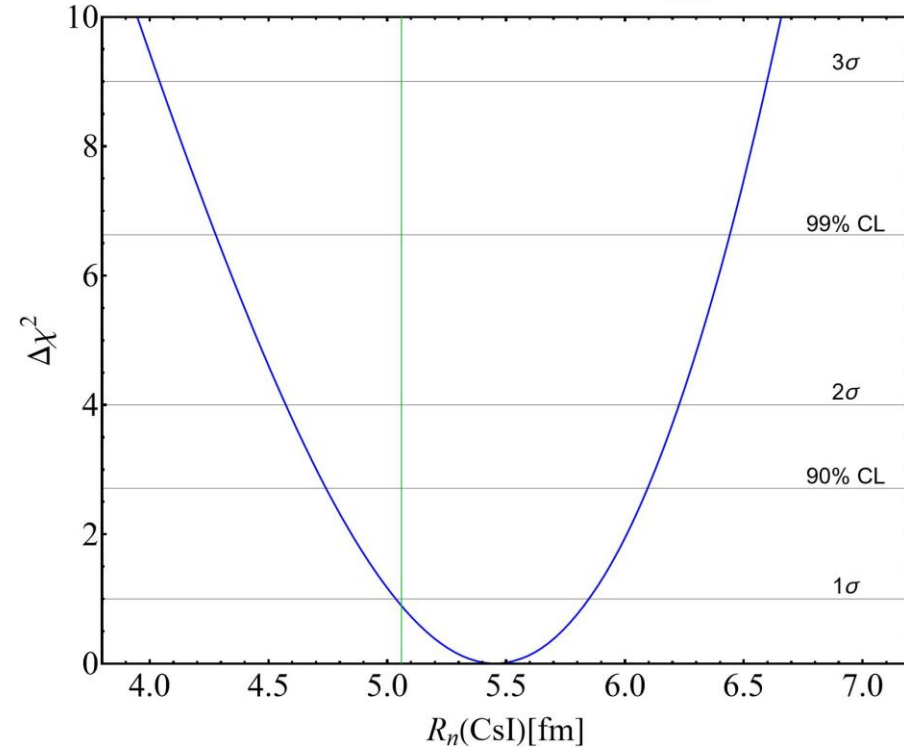
$$R_p(\text{CsI}) \approx 4.78 \text{ fm}$$

$$\Delta R_{np}(\text{CsI}) = 0.69 \pm 0.38 \text{ fm}$$

~7% precision

$$R_n(\text{CsI}) = 5.47 \pm 0.38 \text{ fm} \quad \chi^2_{\min} = 85.2$$

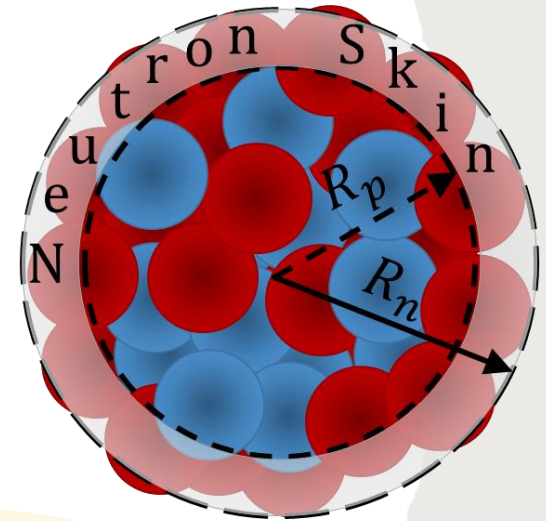
See also D.
Papoulias's
talk



Only an averaged
information is obtained,
could we do more?



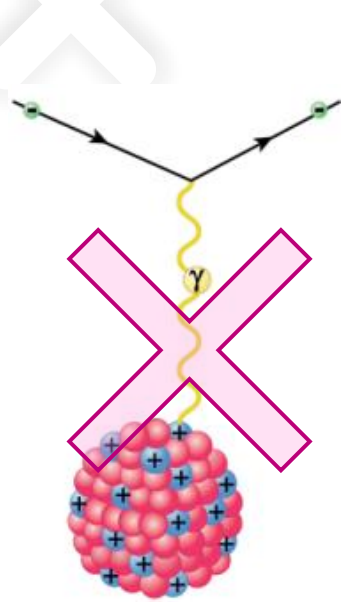
Use another electroweak
process that measures the
weak charge of Cs



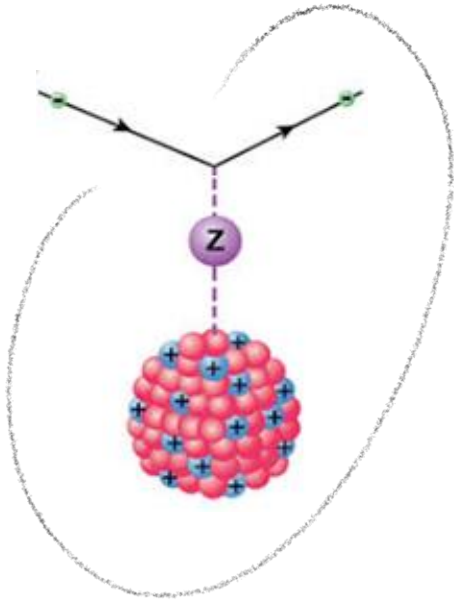
$$R_n(\text{COH} - \text{CsI}) = 5.47^{+0.38}_{-0.38}(1\sigma)^{+0.63}_{-0.72}(90\% \text{CL})^{+0.76}_{-0.89}(2\sigma) \text{ fm},$$

Atomic Parity Violation in cesium APV(Cs)

☐ M. Cadeddu and F. Dordei, PRD 99, 033010 (2019), arXiv:1808.10202



Interaction mediated by the photon and so mostly sensitive to the charge (proton) distribution



Interaction mediated by the Z boson and so mostly sensitive to the weak (neutron) distribution.

+ Parity violation in an atomic system can be observed as an **electric dipole transition amplitude between two atomic states with the same parity**, such as the 6S and 7S states in cesium.

➤ Indeed, a transition between two atomic states with same parity is forbidden by the parity selection rule and cannot happen with the exchange of a photon.

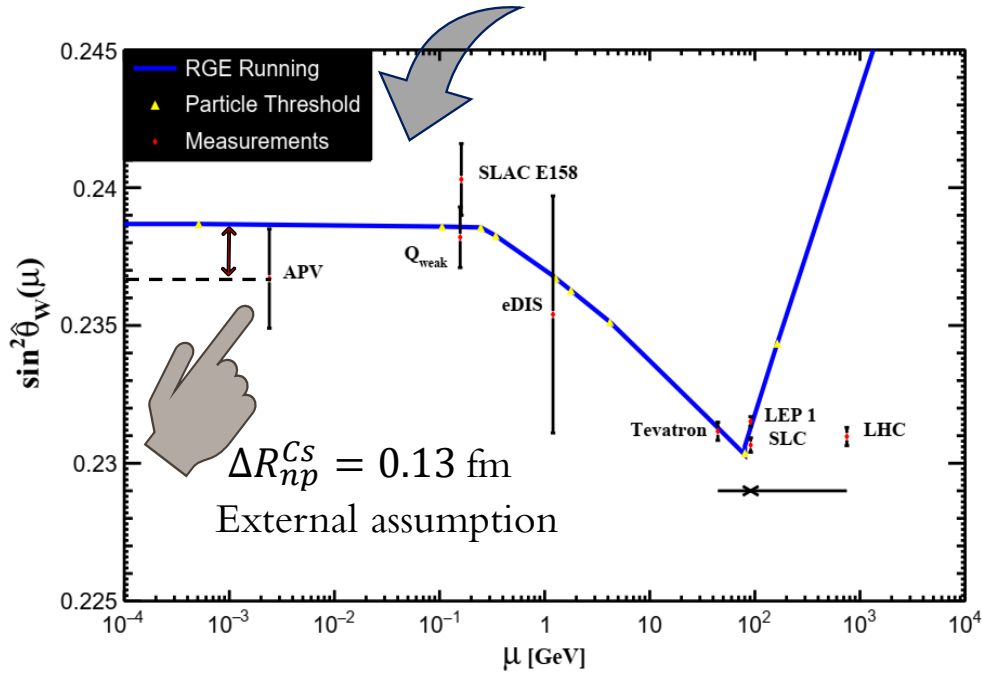
✓ However, an electric dipole transition amplitude can be induced by a Z boson exchange between atomic electrons and nucleons → Atomic Parity Violation (APV) or Parity Non Conserving (PNC).

+ The quantity that is measured is the usual **weak charge**

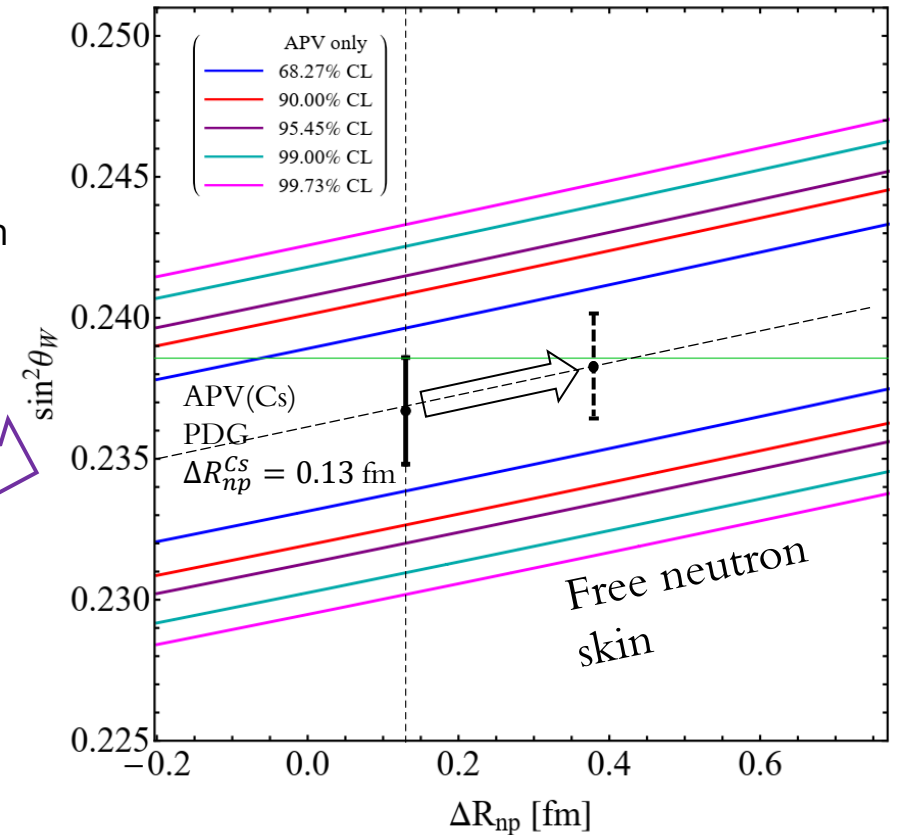
$$Q_W^{SM} \approx Z(1 - 4 \sin^2 \theta_W^{SM}) - N$$

Weak mixing angle from APV(Cs)

Historically APV(Cs) has been used to extract the **lowest energy determination of the weak mixing angle**.



However $R_n(Cs)$ (or the neutron skin) has been taken from **indirect measurements** using antiprotonic atoms, which are known to be affected by considerable model dependencies



✓ The theoretical PNC amplitude of the electric dipole transition is calculated from atomic theory to be

$$\text{Im } E_{\text{PNC}} = (0.8977 \pm 0.0040) \times 10^{-11} |e| a_B Q_W / N$$

Value of $\text{Im } E_{\text{PNC}}$ used by PDG (V. Dzuba *et al.*, PRL 109, 203003 (2012))

I will refer to it with "APV PDG".

But, we also use NEW result on $\text{Im } E_{\text{PNC}}$!

B. K. Sahoo *et al.* PRD 103, L111303 (2021)



I will refer to **APV 2021** when using $\text{Im } E_{\text{PNC}}$ from Sahoo *et al.*

1D fits

R_n fixed to theory*

$R_n^{NSM}(\text{CsI}) \approx 5.06 \text{ fm}$

$\sin^2 \vartheta_W$ free to vary

* Nuclear shell model

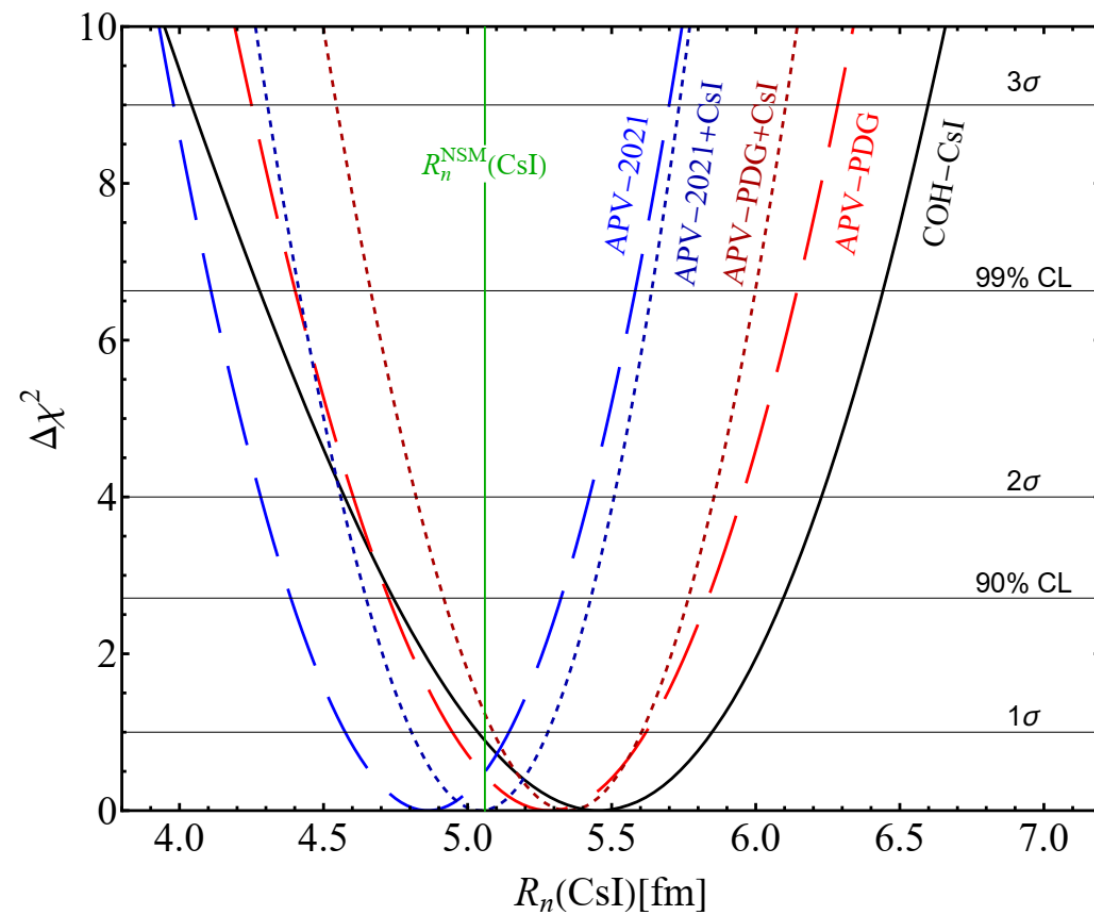
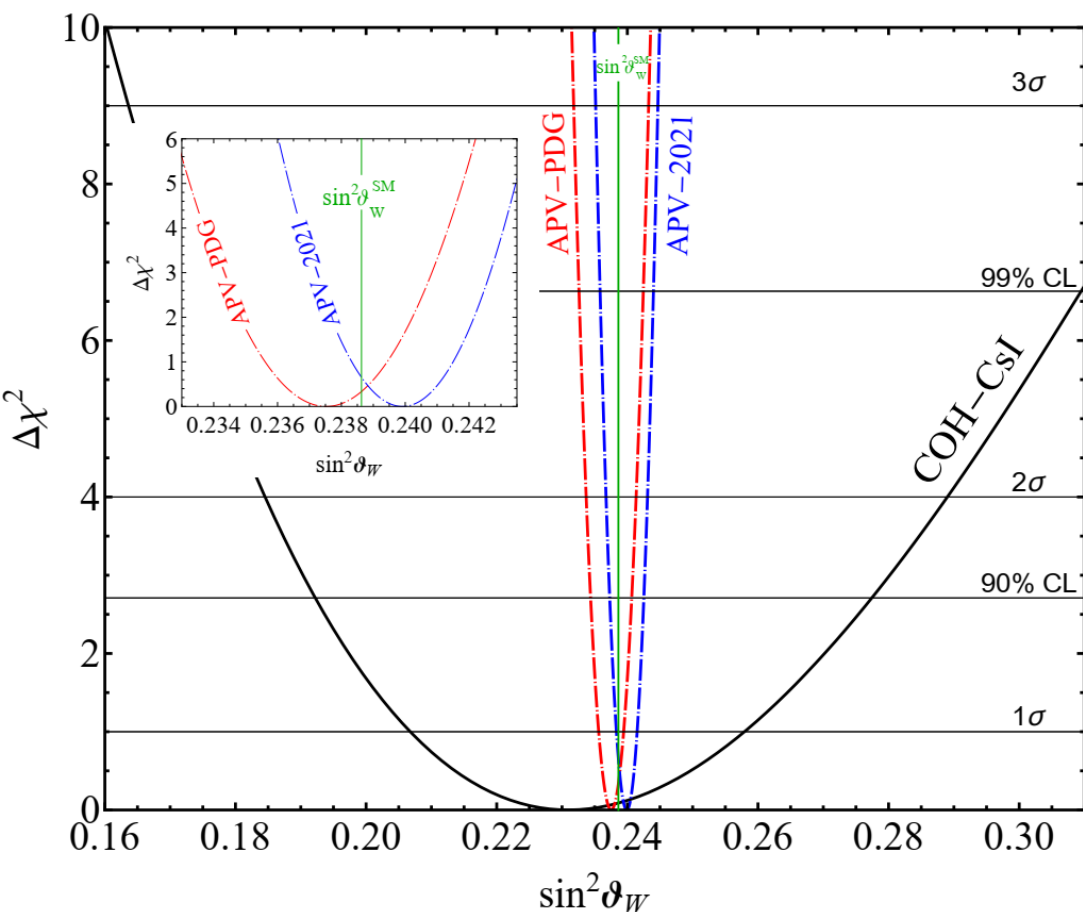


	$\sin^2 \vartheta_W$	χ^2_{\min}	$R_n(\text{CsI})[\text{fm}]$	χ^2_{\min}
	best-fit ^{+1σ+90%CL+2σ} -1σ-90%CL-2σ		best-fit ^{+1σ+90%CL+2σ} -1σ-90%CL-2σ	
COH-CsI	0.231 ^{+0.027+0.046+0.058} -0.024-0.039-0.047	86.0	5.47 ^{+0.38+0.63+0.76} -0.38-0.72-0.89	85.2
APV PDG	0.2375 ^{+0.0019+0.0031+0.0038} -0.0019-0.0031-0.0038	-	5.29 ^{+0.33+0.55+0.66} -0.34-0.56-0.68	-
APV 2021	0.2399 ^{+0.0016+0.0026+0.0032} -0.0016-0.0026-0.0032	-	4.86 ^{+0.28+0.46+0.56} -0.29-0.48-0.58	-
APV PDG + CsI	0.2374 ^{+0.0020+0.0032+0.0039} -0.0018-0.0031-0.0037	86.0	5.35 ^{+0.25+0.41+0.50} -0.26-0.43-0.53	85.3
APV 2021 + CsI	0.2398 ^{+0.0016+0.0026+0.0032} -0.0015-0.0026-0.0031	86.0	5.04 ^{+0.23+0.38+0.46} -0.24-0.40-0.48	86.6

$\sin^2 \vartheta_W$ fixed to theory

$\sin^2 \hat{\theta}_W(0) = 0.23863(5)$

R_n free to vary

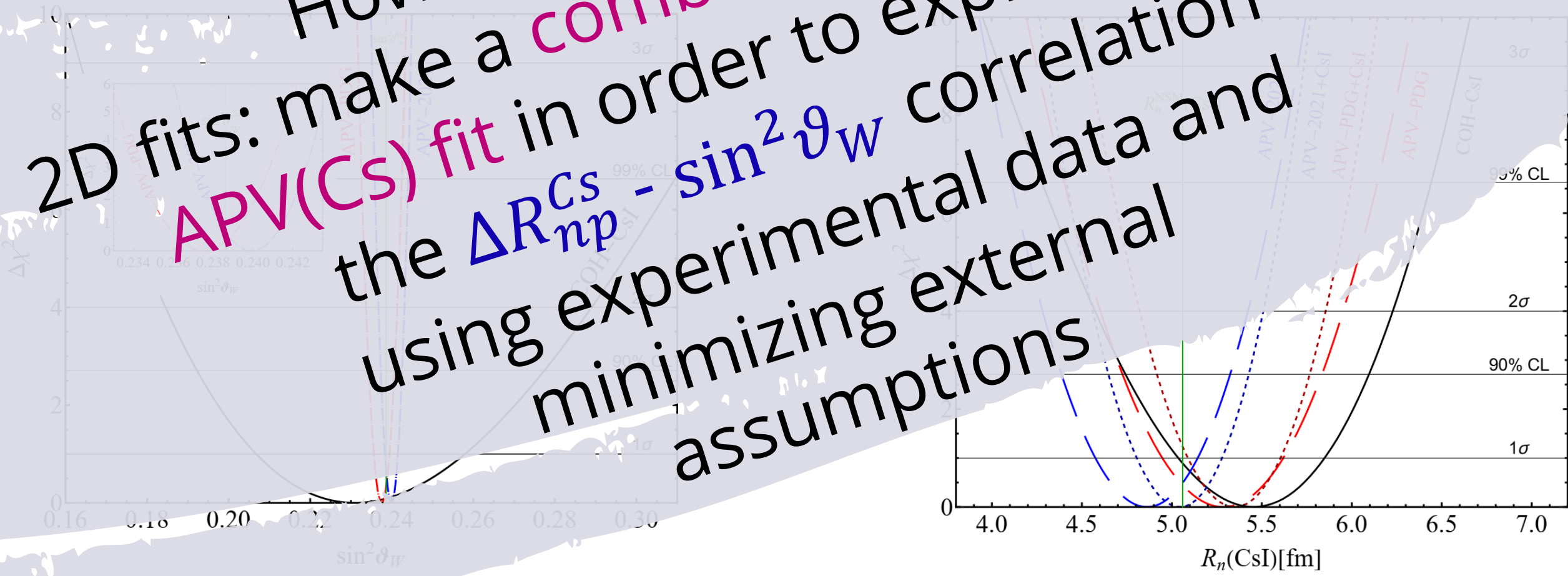


R_n fixed to theory*
 $\sin^2 \vartheta_W$ free to vary

R_n fixed to theory*
 $\sin^2 \vartheta_W$ free to vary

However, we can do more!

2D fits: make a combined $\Delta R_{np}^{Cs} - \sin^2 \vartheta_w$ fit in order to explore the correlation using experimental data and minimizing external assumptions



1st advantage: $R_n(Cs)$ & $R_n(I)$ separation

Even if theoretical nuclear models predict a similar neutron radius for Cs and I, i.e. $R_n(Cs) = 5.09 \text{ fm} \approx R_n(I) = 5.03 \text{ fm}$, meaning that the use of $R_n(CsI)$ is OK for current precision, it is interesting to try to separate the cesium and iodine contributions.

Assuming to know the value of the weak mixing angle at low energy $\sin^2 \hat{\theta}_W(0) = 0.23863(5)$

$$R_n(Cs) = 5.29^{+0.31}_{-0.34} \text{ fm} \quad R_n(I) = 5.6^{+1.0}_{-0.8} \text{ fm} \quad \chi^2_{\min} = 85.2$$

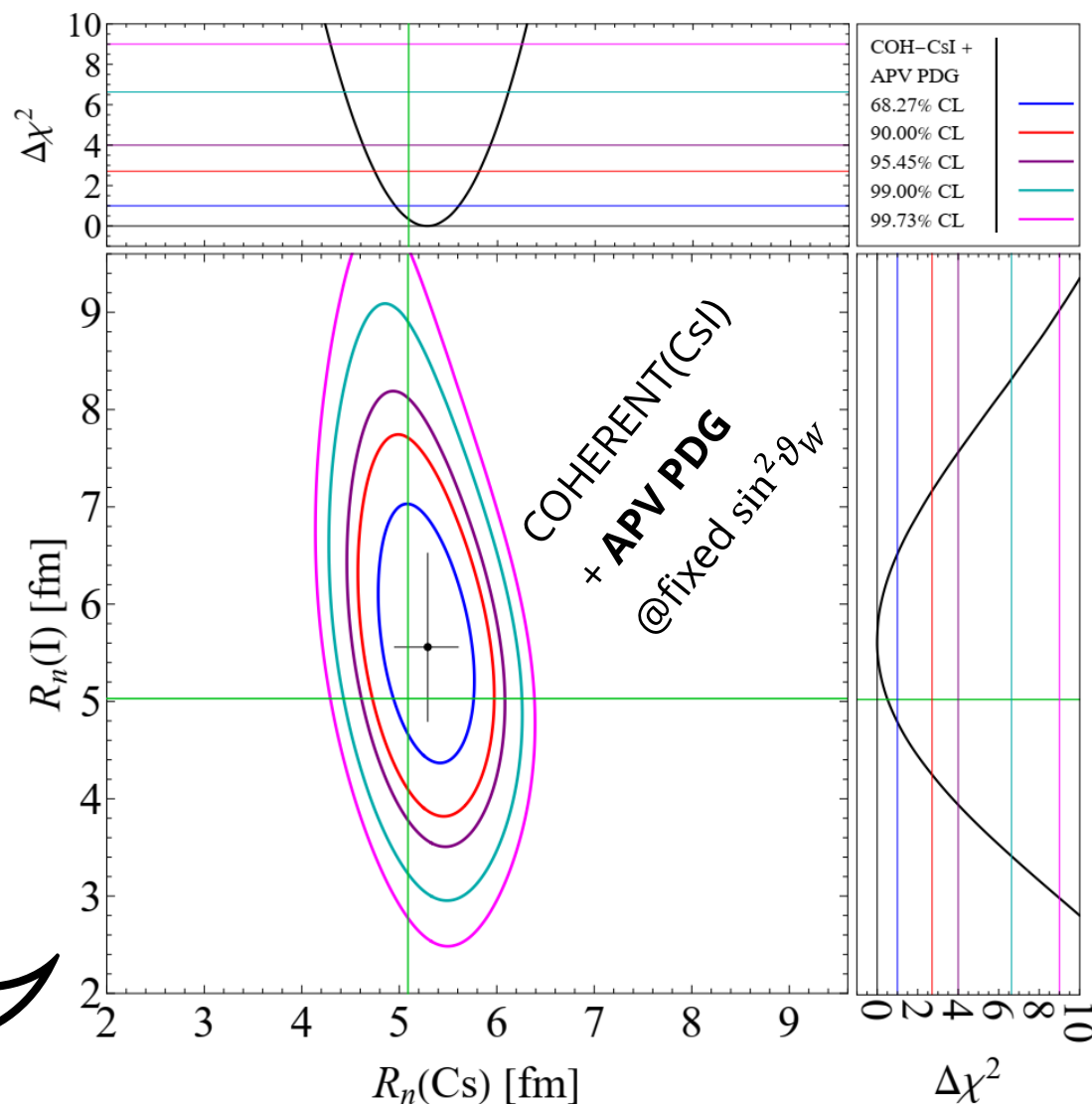
$$\chi^2 = \chi_C^2 + \left(\frac{Q_W^{\text{Cs ns}}(R_n) - Q_W^{\text{th}}(\sin^2 \vartheta_W)}{\sigma_{\text{APV}}(R_n, \sin^2 \vartheta_W)} \right)^2$$

↓ COHERENT χ^2 ↓ APV χ^2

$$\Delta R_{np}(^{127}\text{I}) = R_n - R_p = 0.57^{+1.0}_{-0.8} \text{ fm}$$

$$\Delta R_{np}(^{133}\text{Cs}) = R_n - R_p = 0.2^{+0.31}_{-0.34} \text{ fm}$$

Contribution of Cs and I disentangled!!



1st advantage: $R_n(Cs)$ & $R_n(I)$ separation

$$R_n(Cs)=4.85^{+0.30}_{-0.25} \text{ fm} \quad R_n(I)=6.0^{+0.9}_{-0.9} \text{ fm} \quad \chi^2_{\min}=85.3$$

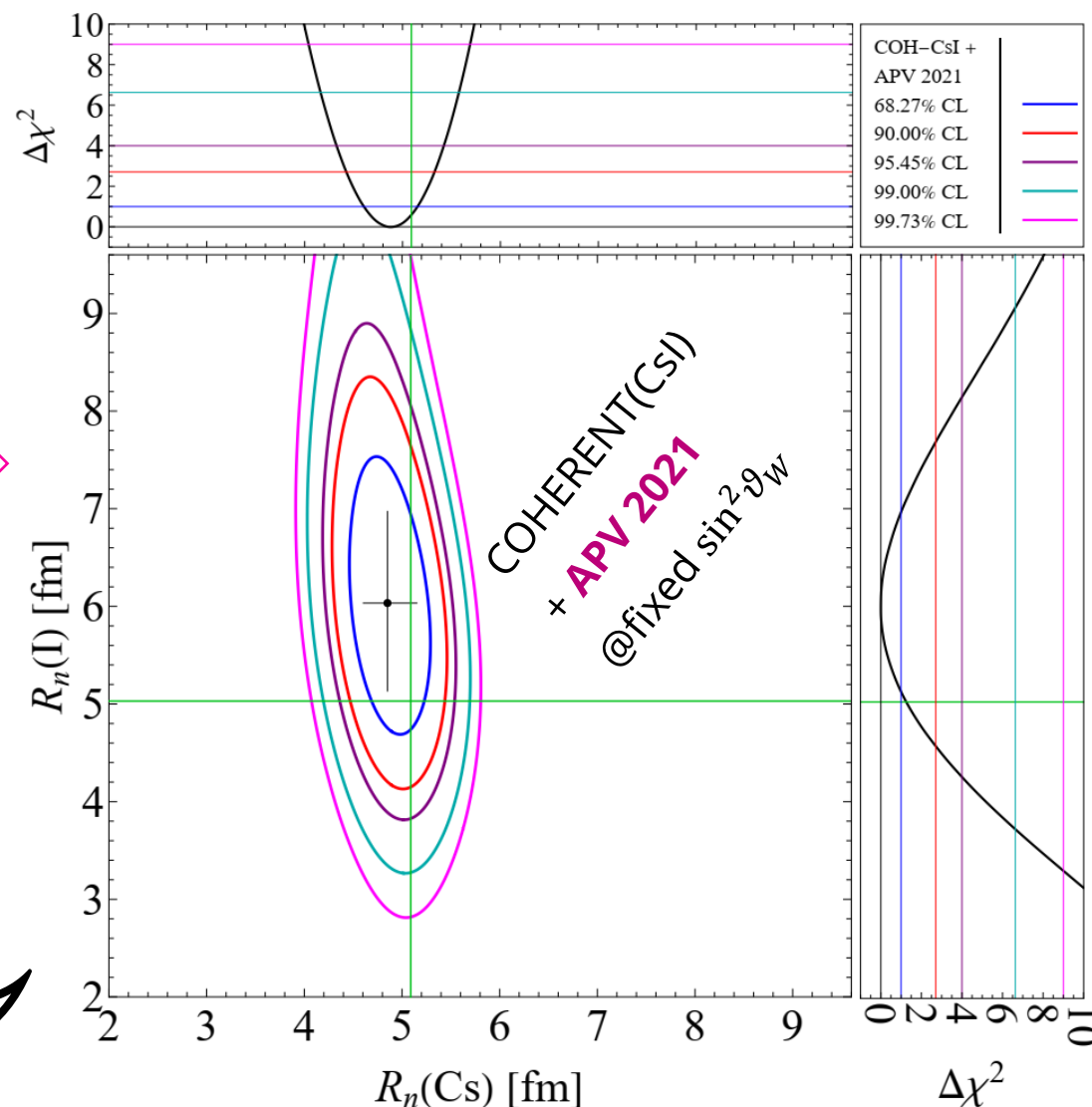
Even if theoretical nuclear models predict a similar neutron radius for Cs and I, i.e. $R_n(Cs) = 5.09 \text{ fm} \approx R_n(I) = 5.03 \text{ fm}$, meaning that the use of $R_n(CsI)$ is OK for current precision, it is interesting to try to separate the cesium and iodine contributions.

Using $\text{Im}E_{PNC}$ form B. K. Sahoo et al.
PRD 103, L111303 (2021) (**APV 2021**)

$$\Delta R_{np}(^{127}\text{I}) = R_n - R_p = 0.97^{+0.9}_{-0.9} \text{ fm}$$

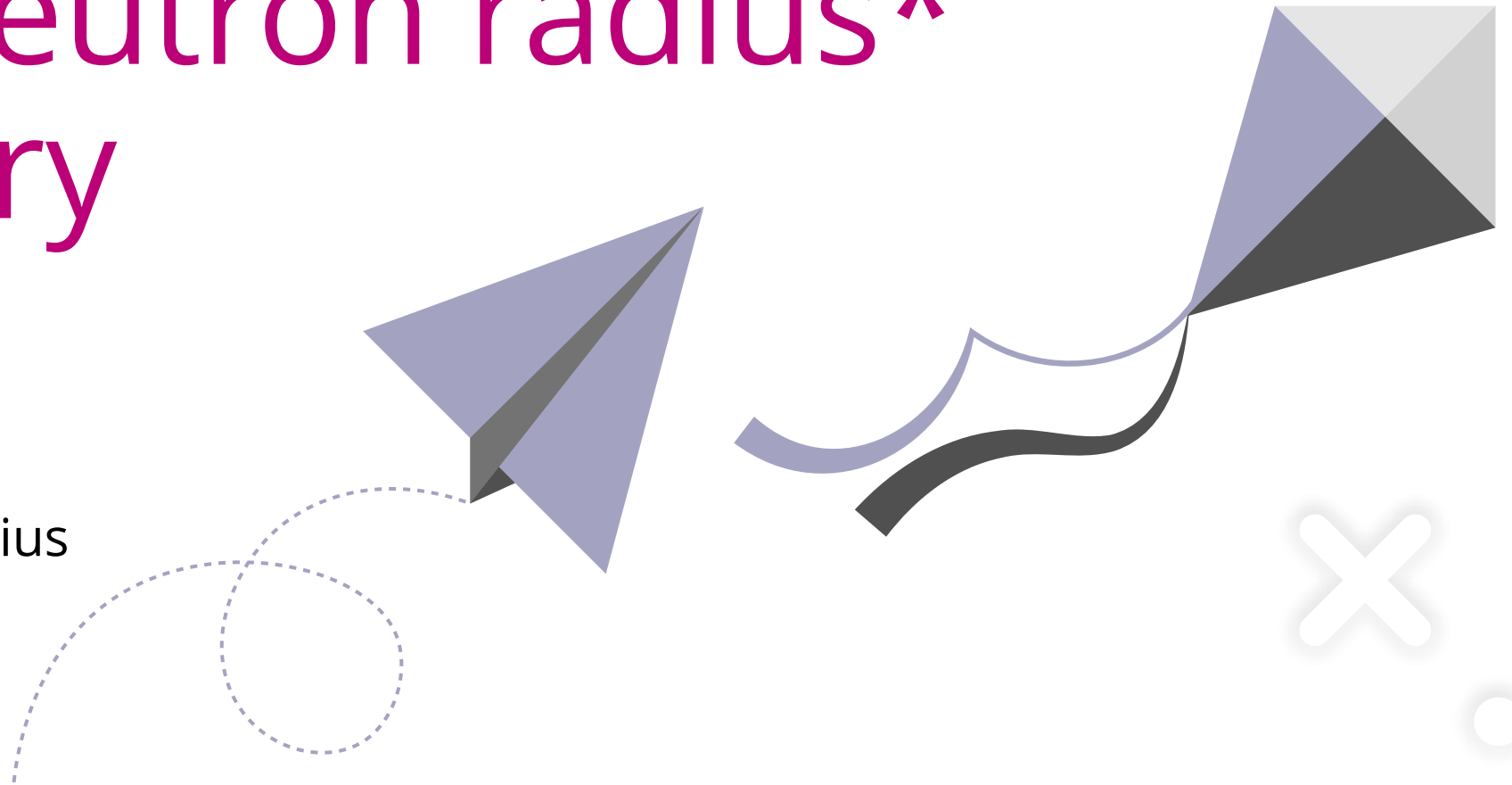
$$\Delta R_{np}(^{133}\text{Cs}) = R_n - R_p = -0.24^{+0.30}_{-0.25} \text{ fm}$$

Contribution of Cs and I disentangled!!



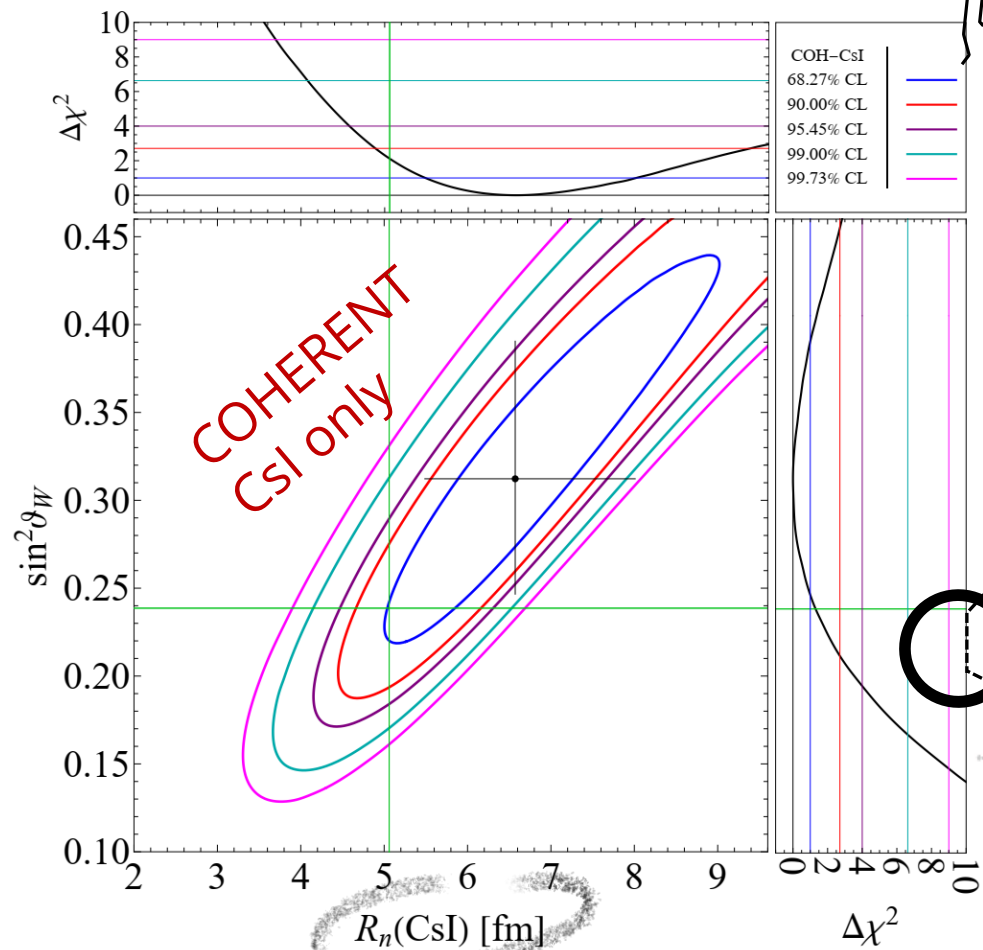
2D fit: leaving both the
weak mixing angle and the
nuclear neutron radius*
free to vary

*average Csl neutron radius



2nd advantage: extract both $R_n(\text{CsI})$ and $\sin^2\vartheta_W$ from data

$$R_n(\text{CsI}) = 6.6^{+1.4}_{-1.1} \text{ fm} \quad \sin^2\vartheta_W = 0.31^{+0.08}_{-0.07} \quad \chi^2_{\min} = 83.9$$

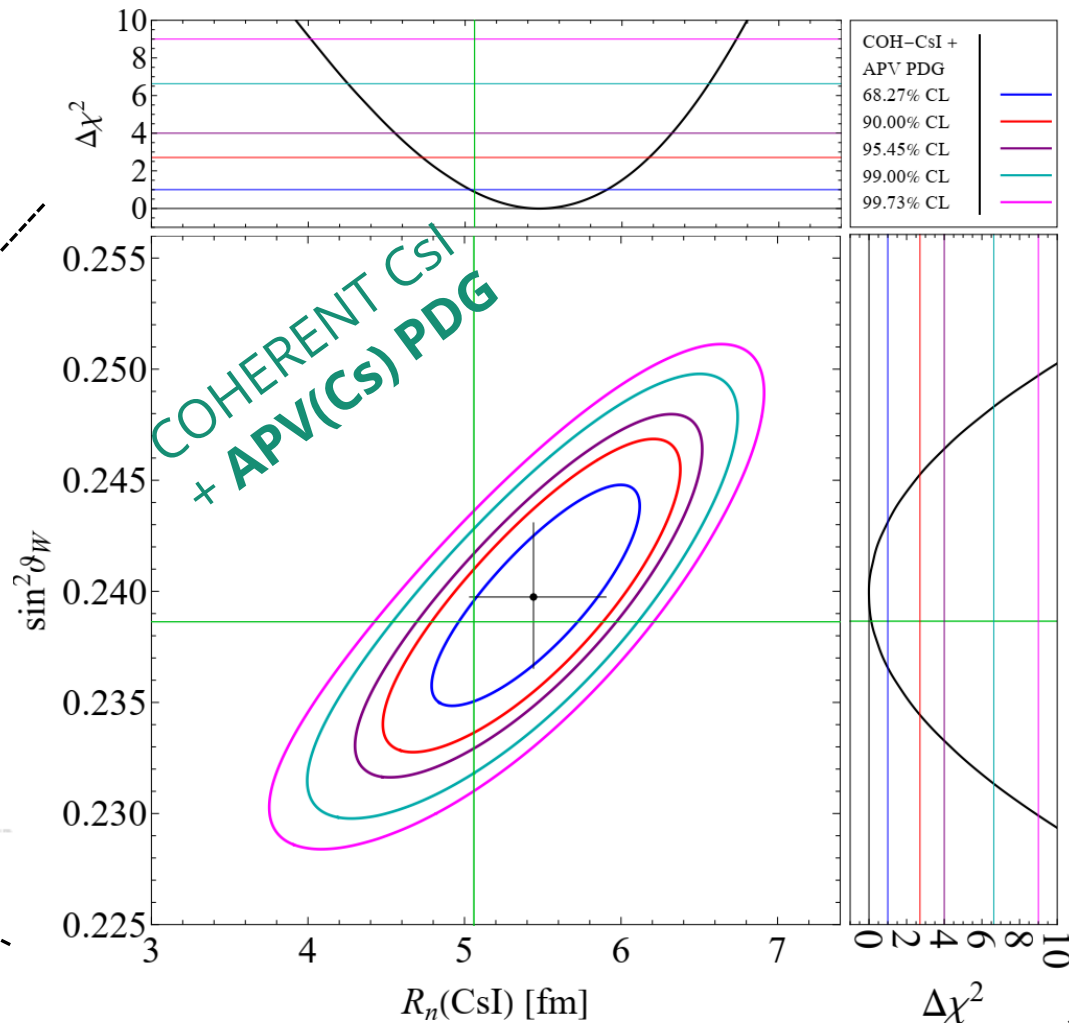


See also D. Papoulias's talk

+APV(Cs)
PDG

MIND THE SCALE

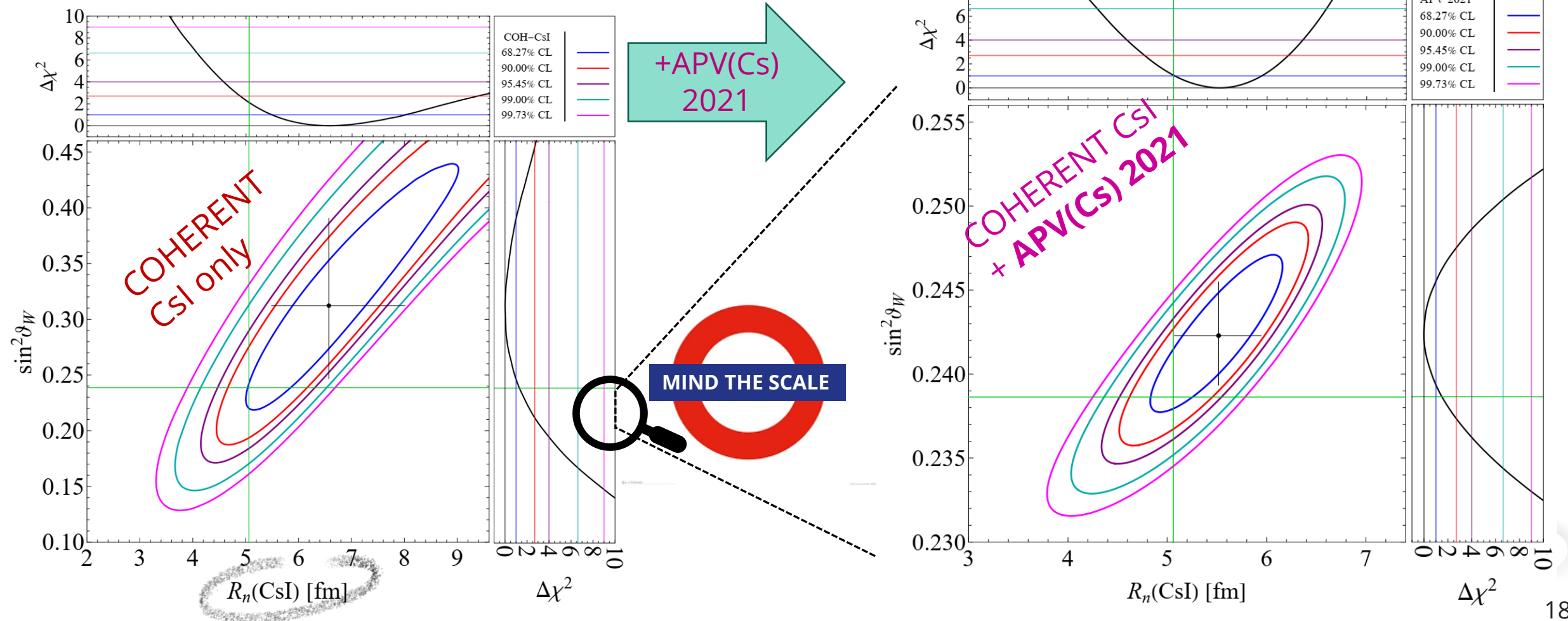
$$R_n(\text{CsI}) = 5.4^{+0.5}_{-0.4} \text{ fm} \quad \sin^2\vartheta_W = 0.2397^{+0.0033}_{-0.0032} \quad \chi^2_{\min} = 85.2$$



2nd advantage: extract both $R_n(\text{CsI})$ & $\sin^2\vartheta_W$ from data

$$R_n(\text{CsI}) = 5.5^{+0.4}_{-0.4} \text{ fm} \quad \sin^2\vartheta_W = 0.2423^{+0.0032}_{-0.0029} \quad \chi^2_{\min} = 85.1$$

$$R_n(\text{CsI}) = 6.6^{+1.4}_{-1.1} \text{ fm} \quad \sin^2\vartheta_W = 0.31^{+0.08}_{-0.07} \quad \chi^2_{\min} = 83.9$$



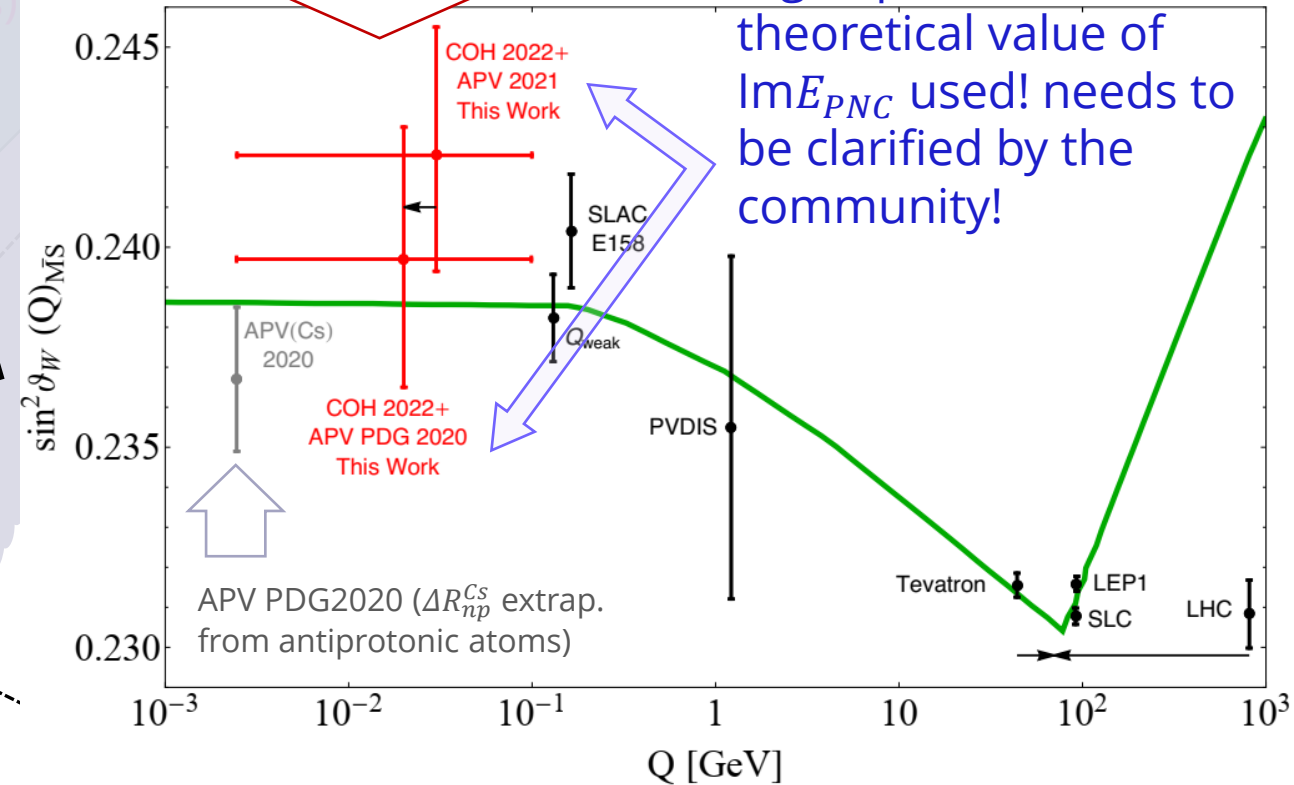
Weak mixing angle determination from APV without any assumption on $R_n(\text{Cs})$

$$R_n(\text{CsI}) = 6.6^{+1.4}_{-1.1} \text{ fm} \quad \sin^2 \theta_W = 0.31^{+0.08}_{-0.07} \quad \chi^2_{\min} = 83.9$$

No assumptions on ΔR_{np}^{Cs} are made. The skin is taken directly from CEvNS experimental data

Big impact due to the theoretical value of $\text{Im} E_{PNC}$ used! needs to be clarified by the community!

👍 We keep almost the same uncertainty as the original APV(Cs) for $\sin^2 \theta_W$ but not assuming a neutron skin value for Cs which instead is driven by CEvNS



Summary of nuclear neutron radius measurements

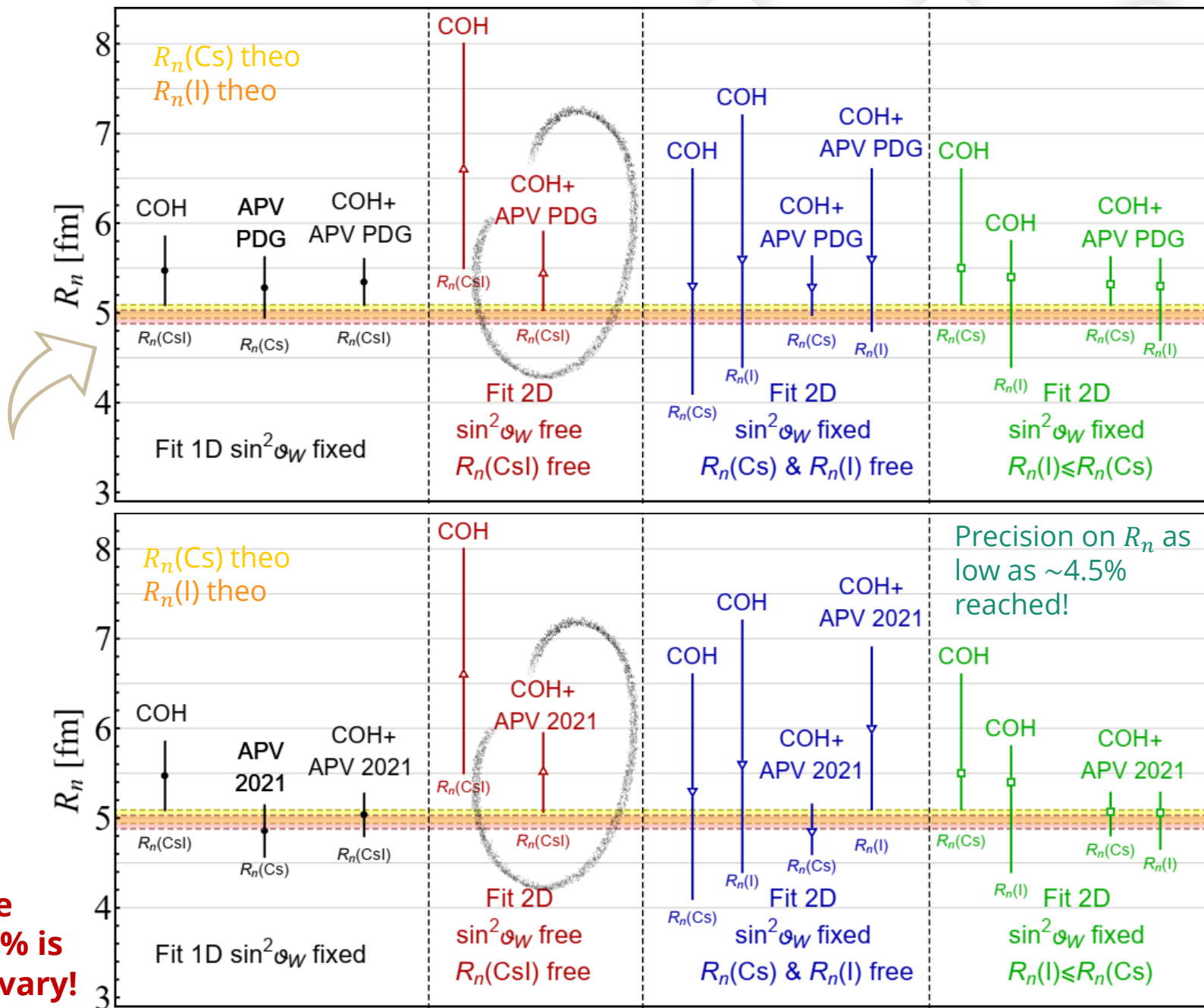
- APV PDG: Using $\text{Im}E_{PNC}$ from V. Dzuba *et al.*, PRL 109, 203003 (2012)

Despite the different fit configurations used to extract the values of $R_n(\text{CsI})$, $R_n(\text{Cs})$ and $R_n(\text{I})$, a coherent picture emerges with an overall agreement between COHERENT and APV results and the theoretical predictions.

Using APV PDG we obtain on average larger values on the radii, still compatible within uncertainties

- APV2021: using $\text{Im}E_{PNC}$ from B. K. Sahoo *et al.* PRD 103, L111303 (2021)

On the contrary, APV 2021 shifts downwards the measured radii towards the predictions, but in the simultaneous 2D fit with $\sin^2\vartheta_W$ where the correlation with the latter increases the extracted central value of $R_n(\text{CsI})$.

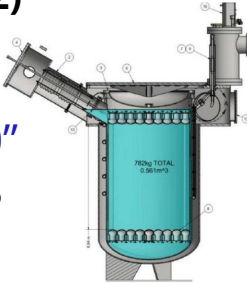


☆☆ 2D fit COHERENT(CsI)+APV(Cs) is stable against $\text{Im}E_{PNC}$ choice. Precision of ~7% is reached even if letting $\sin^2\vartheta_W$ free to vary!

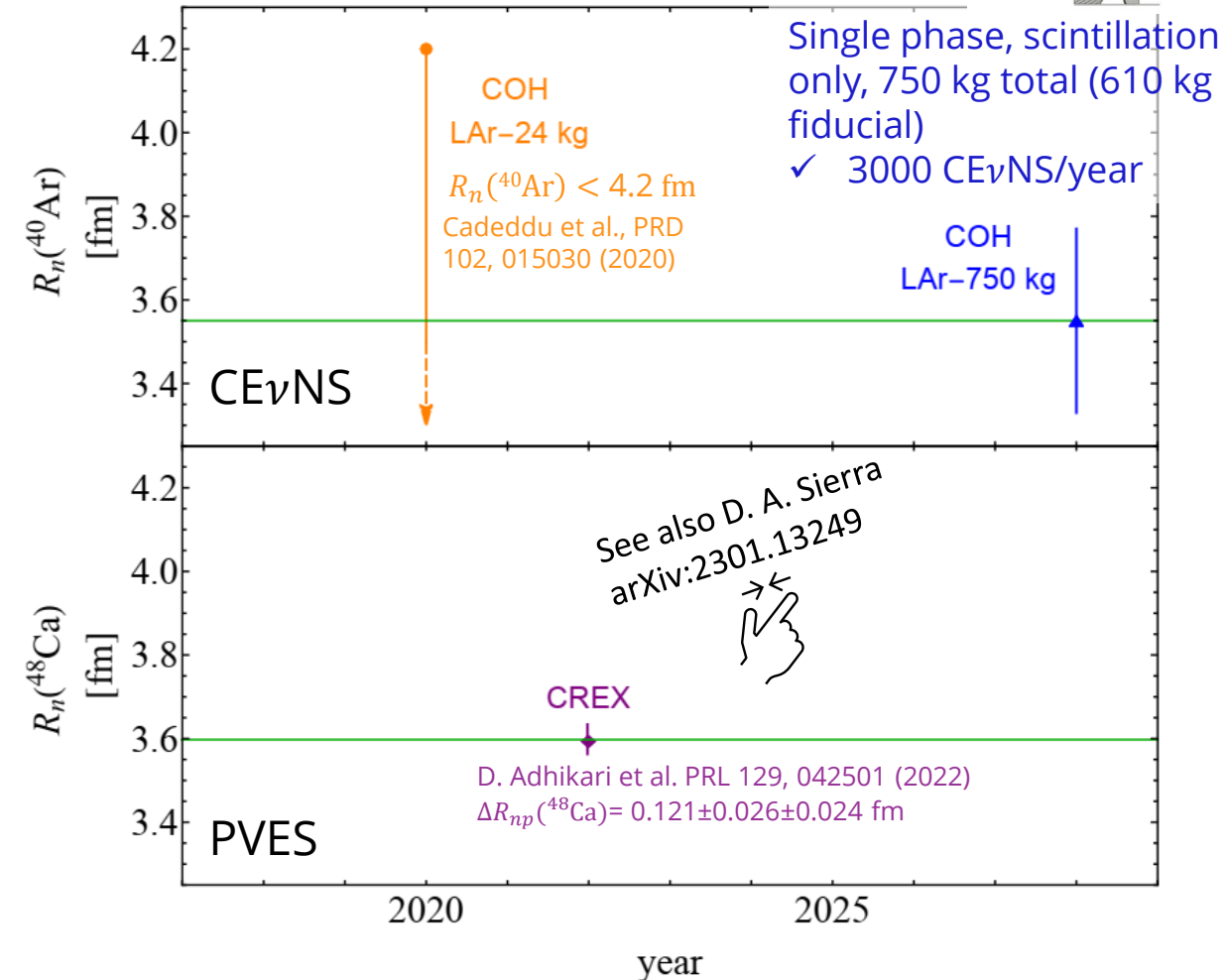
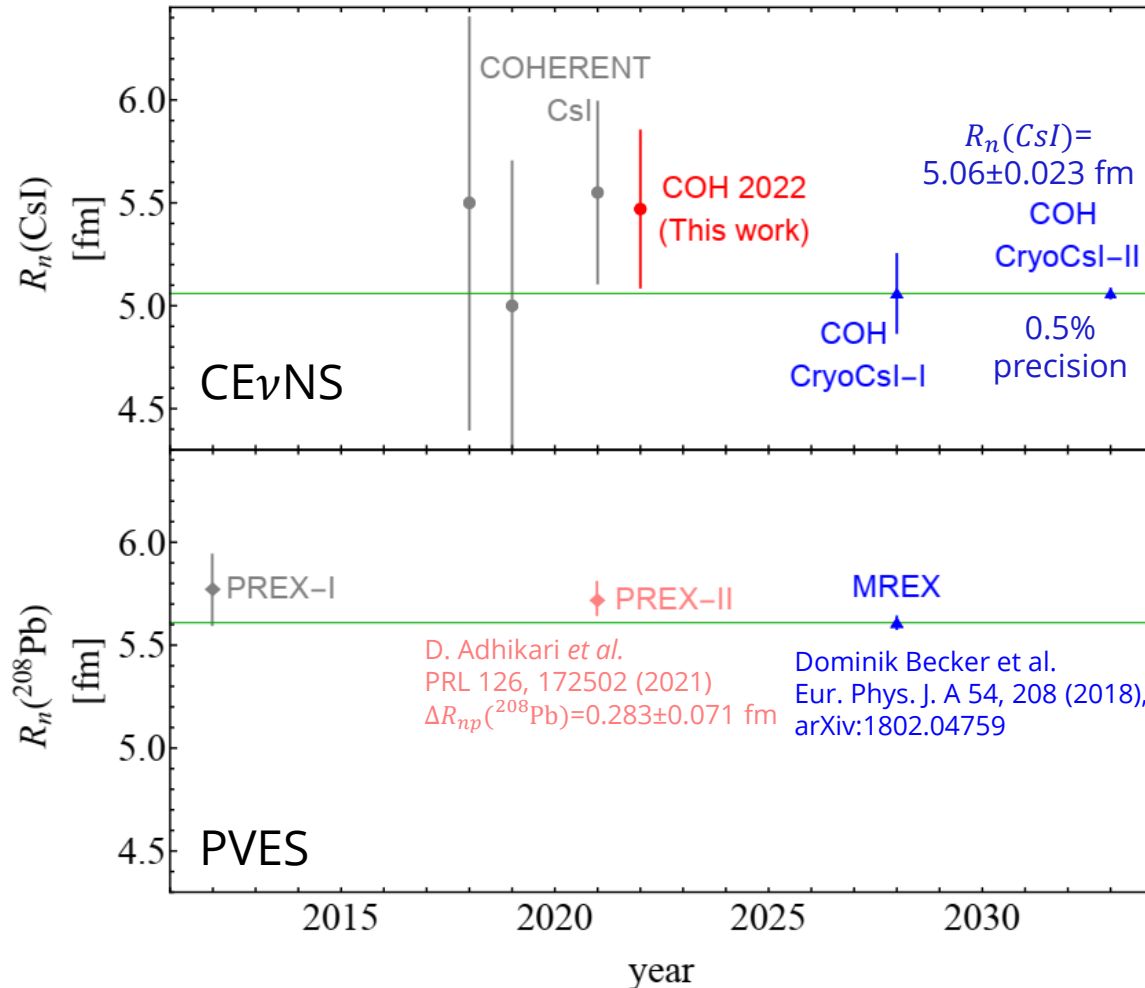
The past, present and future of R_n measurements with $\text{CE}\nu\text{NS}$ and PVES

See details in **D. Akimov et al., arXiv:2204.04575 (2022)**

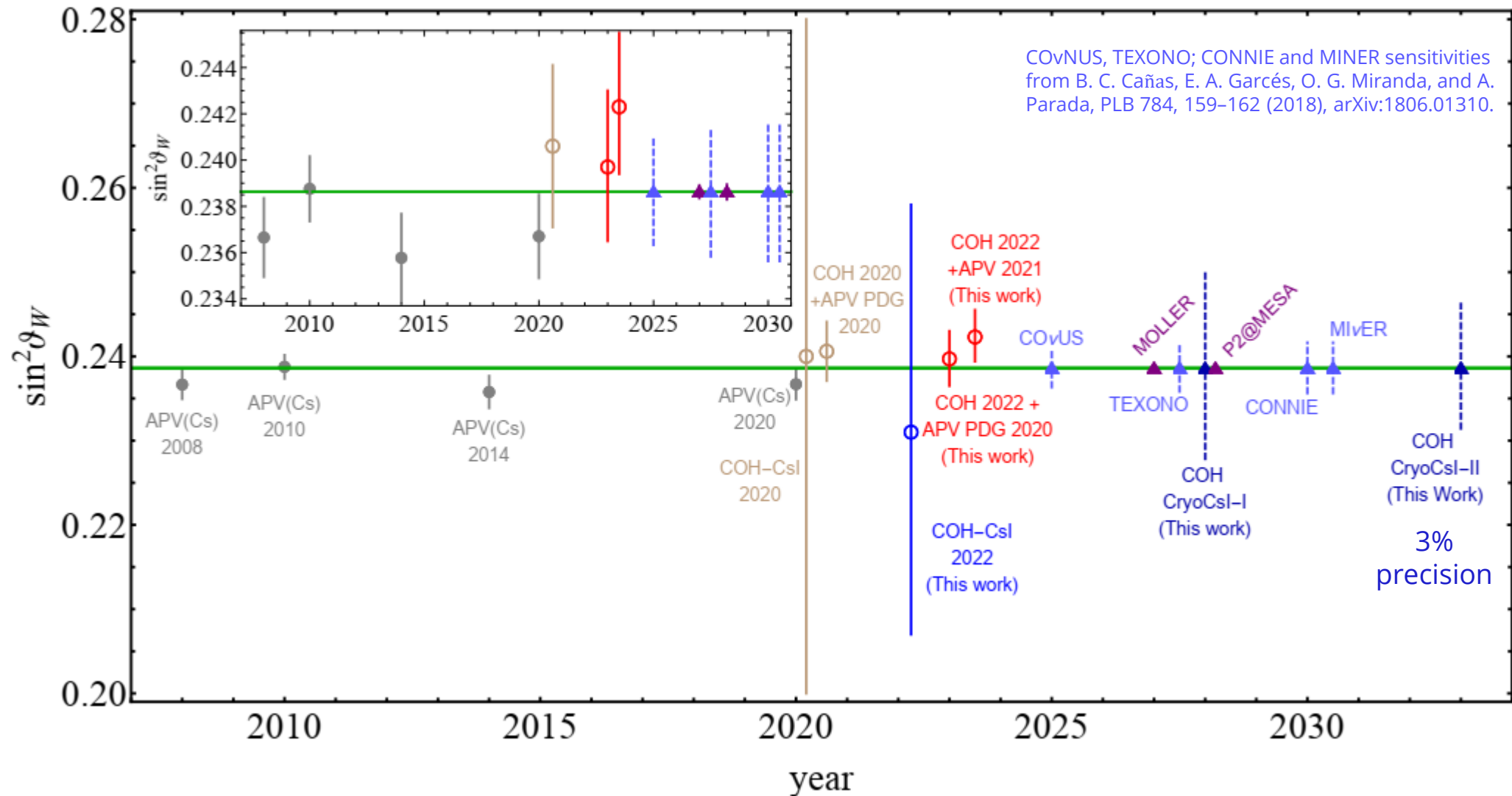
- **COH-CryoCsl-I:** 10 kg, cryogenic temperature ($\sim 40\text{K}$), twice the light yield of present Csl crystal at 300K
- **COH-CryoCsl-II:** 700 kg undoped Csl detector. Both lower energy threshold of 1.4 keVnr while keeping the shape of the energy efficiency of the present COHERENT Csl.



COHERENT future argon: “COH-LAr-750”
LAr based detector for precision $\text{CE}\nu\text{NS}$



The past, present and future of $\sin^2\vartheta_W$ with $\text{CE}\nu\text{NS}$ and APV



Conclusions

- + The **weak-mixing angle-neutron radius degeneracy** is always present in weak processes on nuclei
- + To break this degeneracy one can combine different EW measurements: **Complementarity is the key!**
- + In this game, **CEvNS**, even if not explicitly designed for this purpose, **is a powerful tool** for measuring the neutron form factor (6σ suppression of full coherence reached) that in turn is sensitive to R_n with a precision of 7%.
- + In combination with APV(Cs) a precision **as low as 4.5% in R_n** is obtained and a consistent picture emerges.
- + On the other hand CEvNS is not so sensitive to the $\sin^2\vartheta_W$, but, in combination with APV(Cs) provides **a complete data-driven value of $\sin^2\vartheta_W$** (historically APV uses a R_n (Cs) which is extrapolated)
- + The value of $\sin^2\vartheta_W$ is very dependent on the theoretical $\text{Im } E_{PNC}$ used: needs to be clarified.
- + We provide a complete sensitivity study for future COHERENT experiments in terms of $\sin^2\vartheta_W$ and R_n and we compared it with those coming from parity violation electron scattering showing that a similar precision (0.5%) can be achieved.



The future is bright!





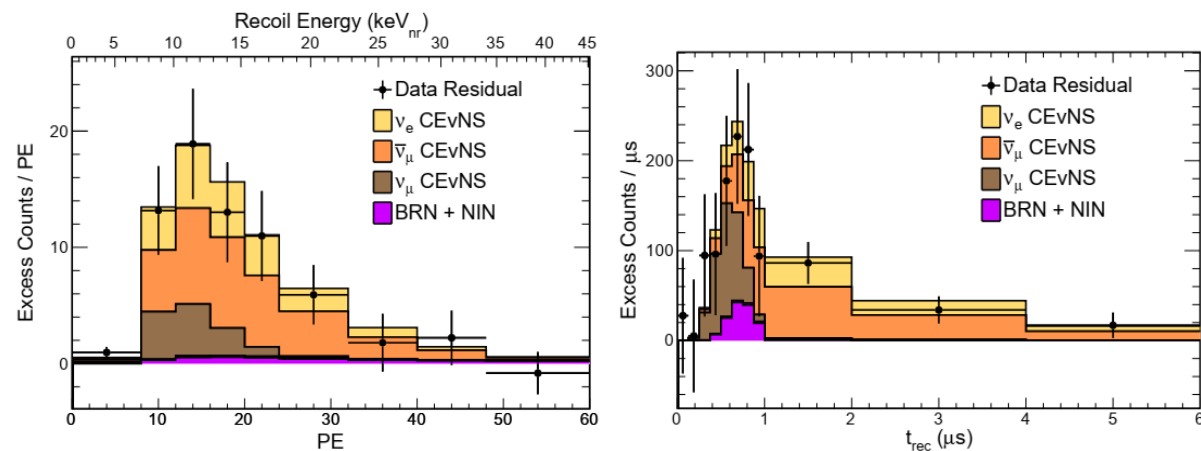
BACKUP

CEvNS players so far

COHERENT CsI

D. Akimov et al. **Science**
357.6356 (2017)

+ Updated in arXiv:2110.07730v1

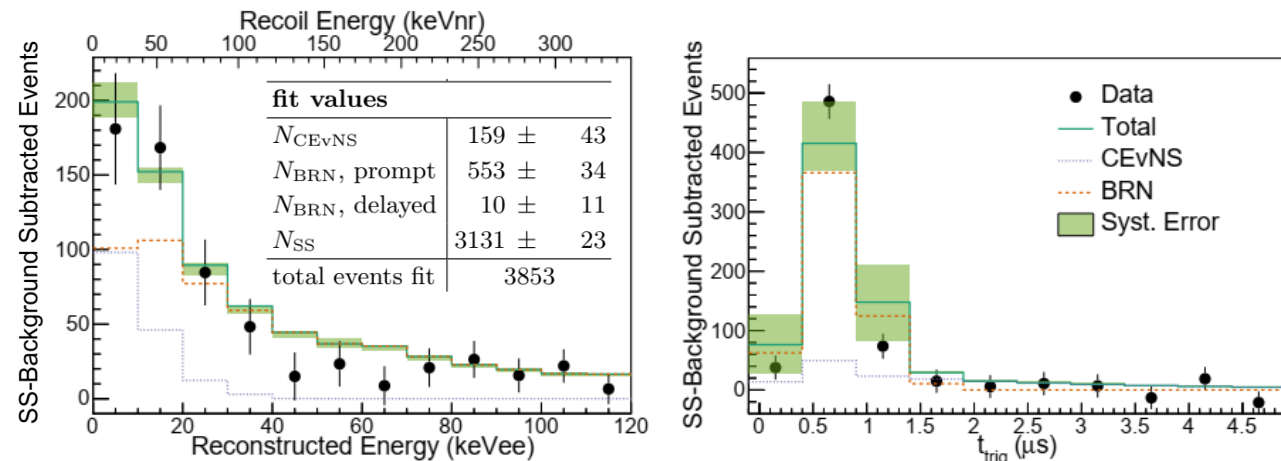


	Prior Prediction	Best-Fit Total
Steady-state background	1286 ± 27	1273 ± 24
BRN	18.4 ± 4.6	17.3 ± 4.5
NIN	5.6 ± 2.0	5.5 ± 2.0
CEvNS	—	306 ± 20

Table I. A summary of prior prediction and best-fit event rates and statistical uncertainties for CEvNS and each background type. The standard-model expectation for CEvNS is $341 \pm 11 \pm 42$.

COHERENT Ar

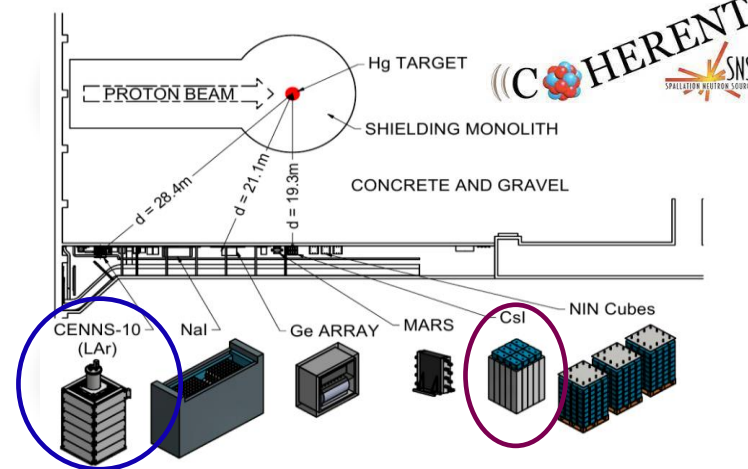
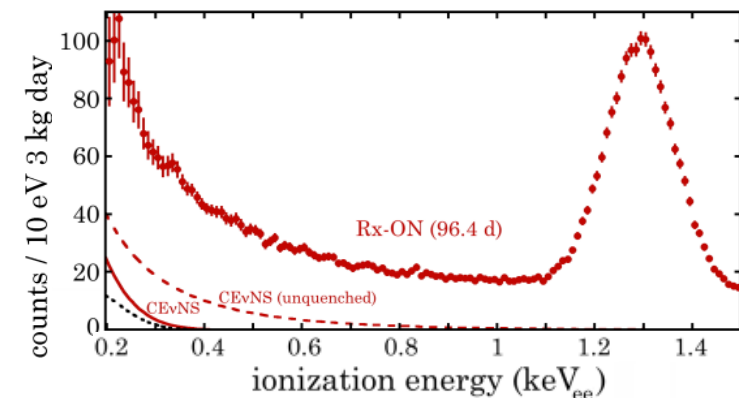
Akimov et al., COHERENT Coll. PRL 126, 01002 (2021)



2022 New player:

Dresden-II

+ 3 kg ultra-low noise germanium detector.
A strong preference for the presence of CEvNS is found.



$F_N(|\vec{q}|^2)$. Thus, in this paper, we calculated the couplings taking into account the radiative corrections in the $\overline{\text{MS}}$ scheme following Refs. [51, 62]

$$\begin{aligned} g_V^{\nu_\ell p} &= \rho \left(\frac{1}{2} - 2 \sin^2 \vartheta_W \right) + 2\mathbb{X}_{WW} + \square_{WW} - 2\varnothing_{\nu_\ell W} + \rho(2\mathbb{X}_{ZZ}^{uL} + \mathbb{X}_{ZZ}^{dL} - 2\mathbb{X}_{ZZ}^{uR} - \mathbb{X}_{ZZ}^{dR}), \\ g_V^{\nu_\ell n} &= -\frac{\rho}{2} + 2\square_{WW} + \mathbb{X}_{WW} + \rho(2\mathbb{X}_{ZZ}^{dL} + \mathbb{X}_{ZZ}^{uL} - 2\mathbb{X}_{ZZ}^{dR} - \mathbb{X}_{ZZ}^{uR}). \end{aligned} \quad (2)$$

The quantities in Eq. (2), \square_{WW} , \mathbb{X}_{WW} and \mathbb{X}_{ZZ}^{fX} , with $f \in \{u, d\}$ and $X \in \{L, R\}$, are the radiative corrections associated with the WW box diagram, the WW crossed-box and the ZZ box respectively, while $\rho = 1.00063$ is a parameter of electroweak interactions. Moreover, $\varnothing_{\nu_\ell W}$ describes the neutrino charge radius contribution and introduces a dependence on the neutrino flavour ℓ (see Ref. [62] or the appendix B of Ref. [63] for further information on such quantities). Numerically, the values of these couplings correspond to $g_V^p(\nu_e) = 0.0382$, $g_V^p(\nu_\mu) = 0.0300$, and $g_V^n = -0.5117$.

COHERENT CsI χ^2

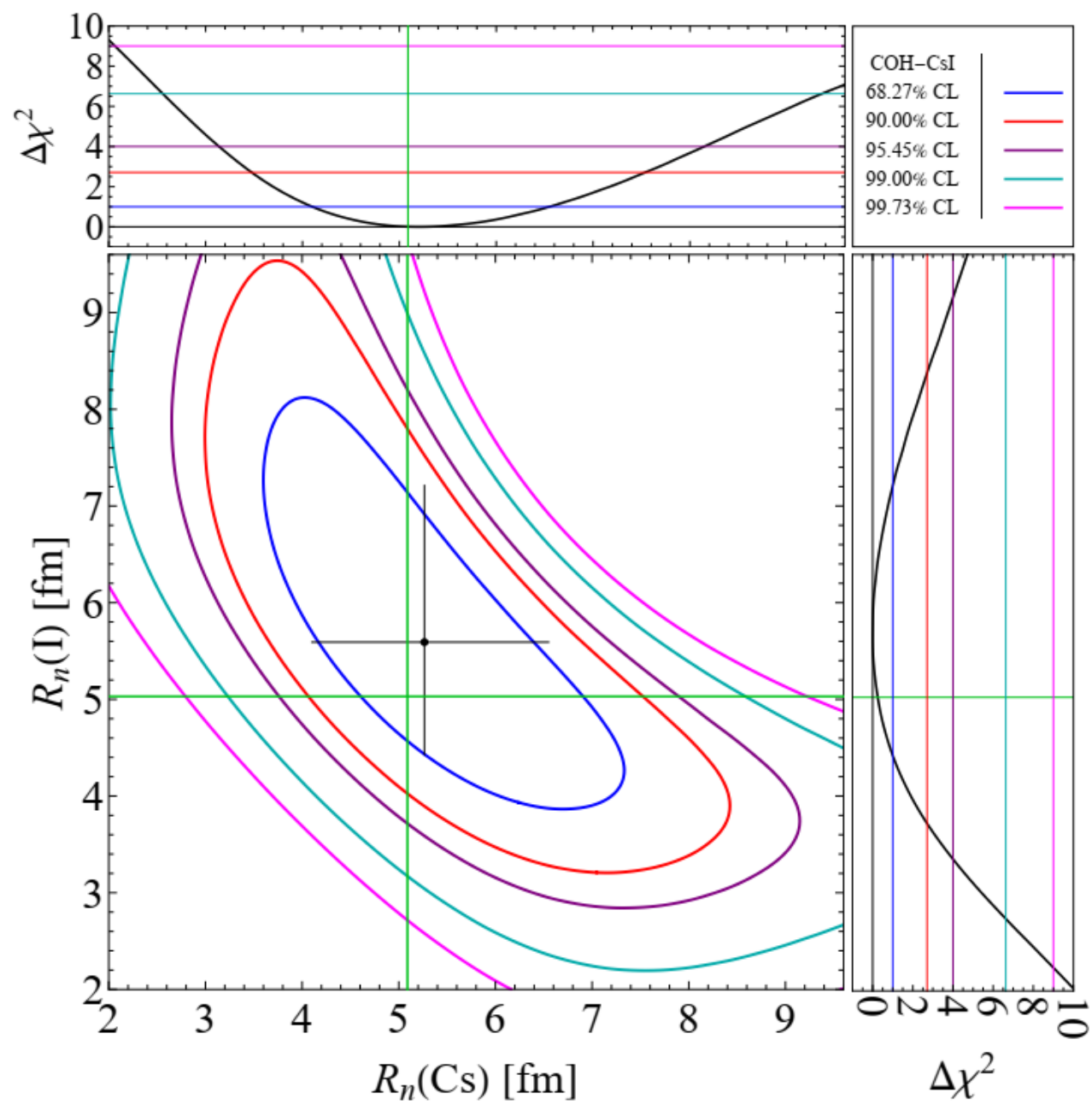
+ Poissonian least-square function:

+ Since in some energy-time bins the number of events is zero, we used the Poissonian least-squares function

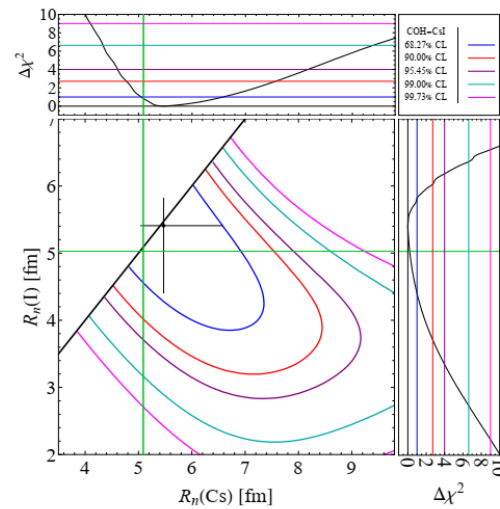
$$\chi_{\text{CsI}}^2 = 2 \sum_{i=1}^9 \sum_{j=1}^{11} \left[\sum_{z=1}^4 (1 + \eta_z) N_{ij}^z - N_{ij}^{\text{exp}} + N_{ij}^{\text{exp}} \ln \left(\frac{N_{ij}^{\text{exp}}}{\sum_{z=1}^4 (1 + \eta_z) N_{ij}^z} \right) \right] + \sum_{z=1}^4 \left(\frac{\eta_z}{\sigma_z} \right)^2, \quad (10)$$

where the indices i, j represent the nuclear-recoil energy and arrival time bin, respectively, while the indices $z = 1, 2, 3, 4$ for N_{ij}^z stand, respectively, for $\text{CE}\nu\text{NS}$, ($N_{ij}^1 = N_{ij}^{\text{CE}\nu\text{NS}}$), beam-related neutron ($N_{ij}^2 = N_{ij}^{\text{BRN}}$), neutrino-induced neutron ($N_{ij}^3 = N_{ij}^{\text{NIN}}$) and steady-state ($N_{ij}^4 = N_{ij}^{\text{SS}}$) backgrounds obtained from the anti-coincidence data. In our notation, N_{ij}^{exp} is the experimental event number obtained from coincidence data and $N_{ij}^{\text{CE}\nu\text{NS}}$ is the predicted number of $\text{CE}\nu\text{NS}$ events that depends on the physics model under consideration, according to the cross-section in Eq. (1), as well as on the neutrino flux, energy resolution, detector efficiency, number of target atoms and the CsI quenching factor [16]. We take into account the systematic uncertainties with the nuisance parameters η_z and the corresponding uncertainties $\sigma_{\text{CE}\nu\text{NS}} = 0.12$, $\sigma_{\text{BRN}} = 0.25$, $\sigma_{\text{NIN}} = 0.35$ and $\sigma_{\text{SS}} = 0.021$ as explained in Refs. [6, 16].

$$R_n(\text{Cs}) = 5.3^{+1.3}_{-1.2} \text{ fm} \quad R_n(\text{I}) = 5.6^{+1.6}_{-1.2} \text{ fm} \quad \chi^2_{\text{min}} = 85.2$$

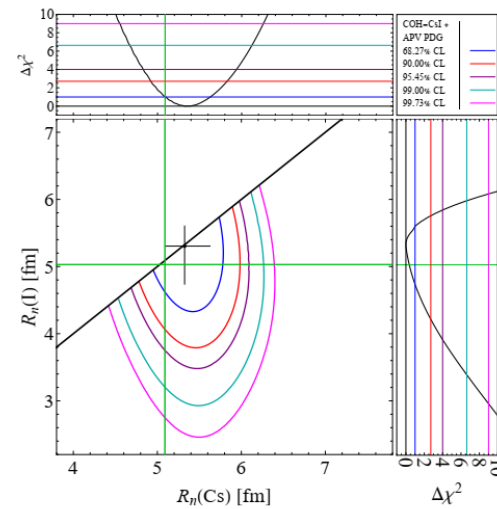


$$R_n(\text{Cs}) = 5.5^{+1.1}_{-0.4} \text{ fm} \quad R_n(\text{I}) = 5.4^{+0.4}_{-1.0} \text{ fm} \quad \chi^2_{\min} = 85.3$$



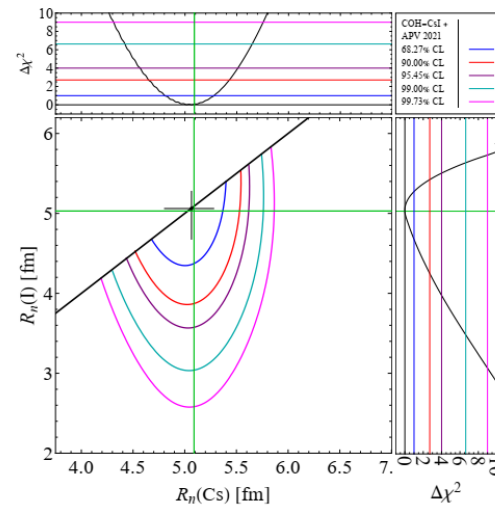
(a)

$$R_n(\text{Cs}) = 5.32^{+0.30}_{-0.23} \text{ fm} \quad R_n(\text{I}) = 5.30^{+0.30}_{-0.6} \text{ fm} \quad \chi^2_{\min} = 85.4$$



(b)

$$R_n(\text{Cs}) = 5.07^{+0.21}_{-0.26} \text{ fm} \quad R_n(\text{I}) = 5.06^{+0.22}_{-0.4} \text{ fm} \quad \chi^2_{\min} = 86.6$$



(c)

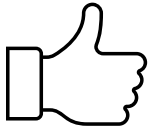
FIG. 10. Constraints on the plane of $R_n(^{133}\text{Cs})$ and $R_n(^{127}\text{I})$ together with their marginalizations, at different CLs obtained fitting the COHERENT CsI data alone (a) and in combination with APV data (b) and (c), using the value for the neutron skin corrections of Ref. [73] (b) and Ref. [74] (c). In all cases, we impose the constraint $R_n(\text{Cs}) \geq R_n(\text{I})$. The green lines indicate the corresponding NSM prediction for the average rms neutron radius of Cs and I.

Dresden-II weak mixing angle results

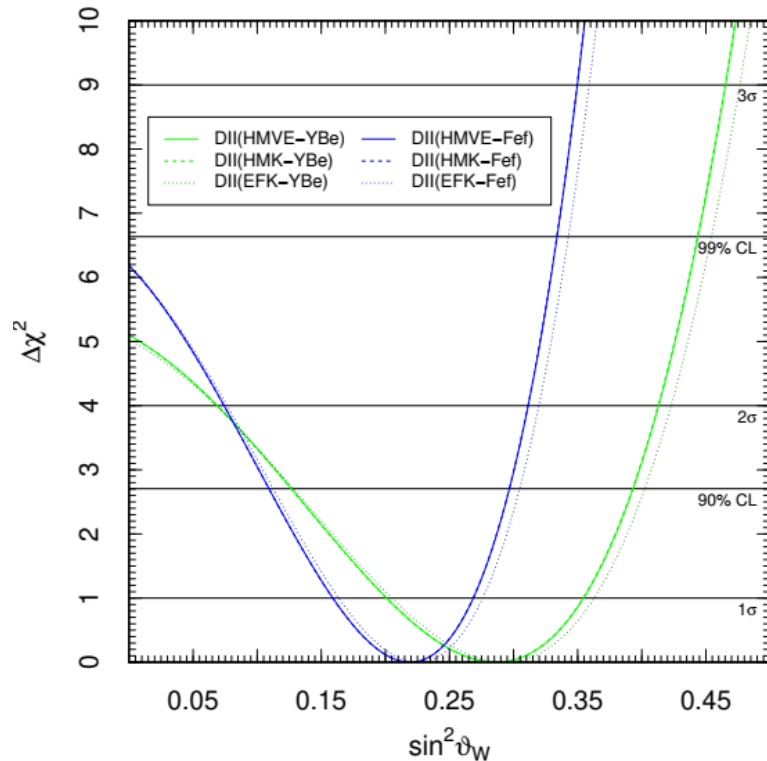
M. Atzori Corona et al., JHEP **09**, 164 (2022), arXiv:2205.09484



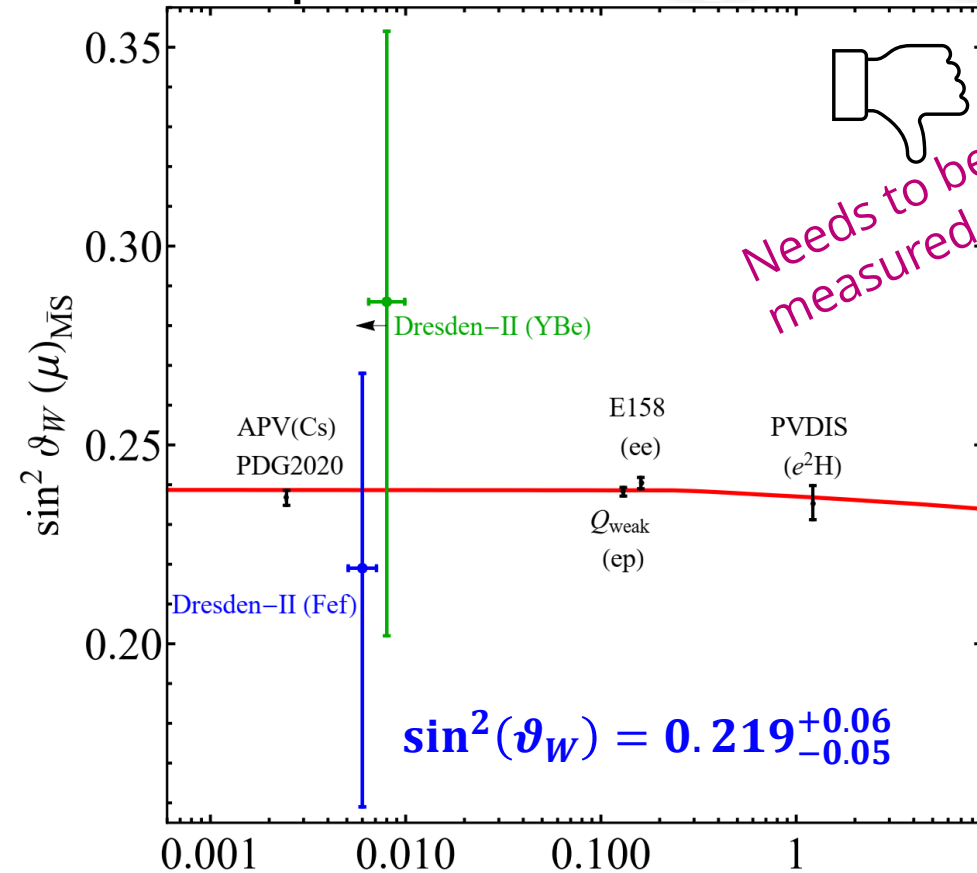
+ Insensitive to $R_n(\text{GeV})$



+ Insensitive to the antineutrino flux parametrization



+ Very sensitive to the Ge quenching factor parametrization

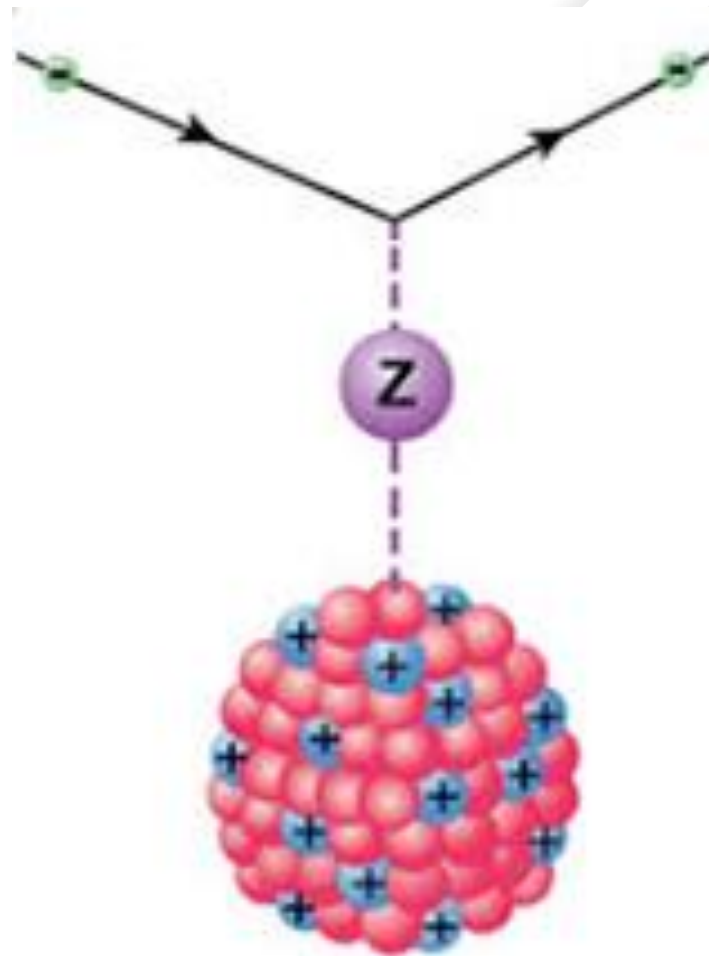
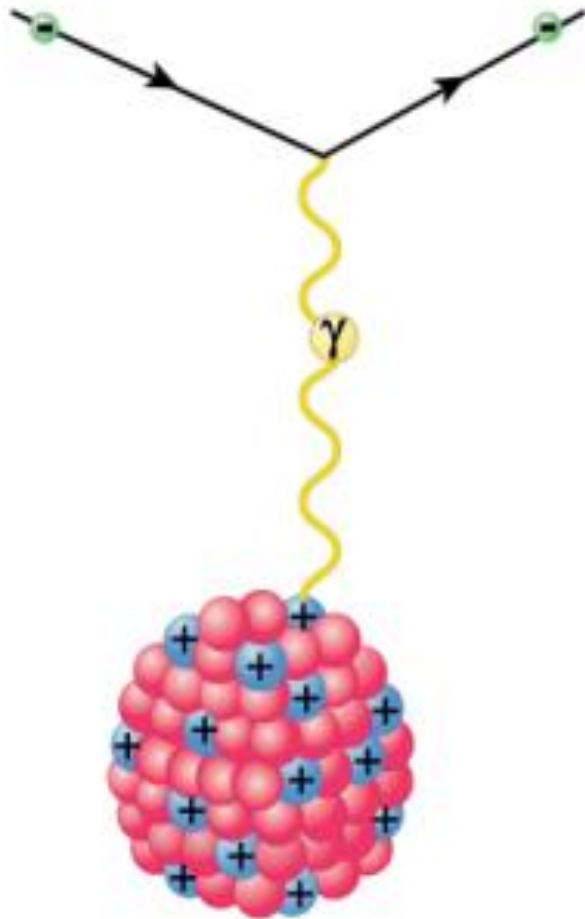


Needs to be accurately measured at low energies

$$\sin^2(\vartheta_W) = 0.219^{+0.06}_{-0.05}$$

See also D. Aristizabal Sierra, V. De Romeri, and D. K. Papoulias, JHEP **09**, 076 (2022)

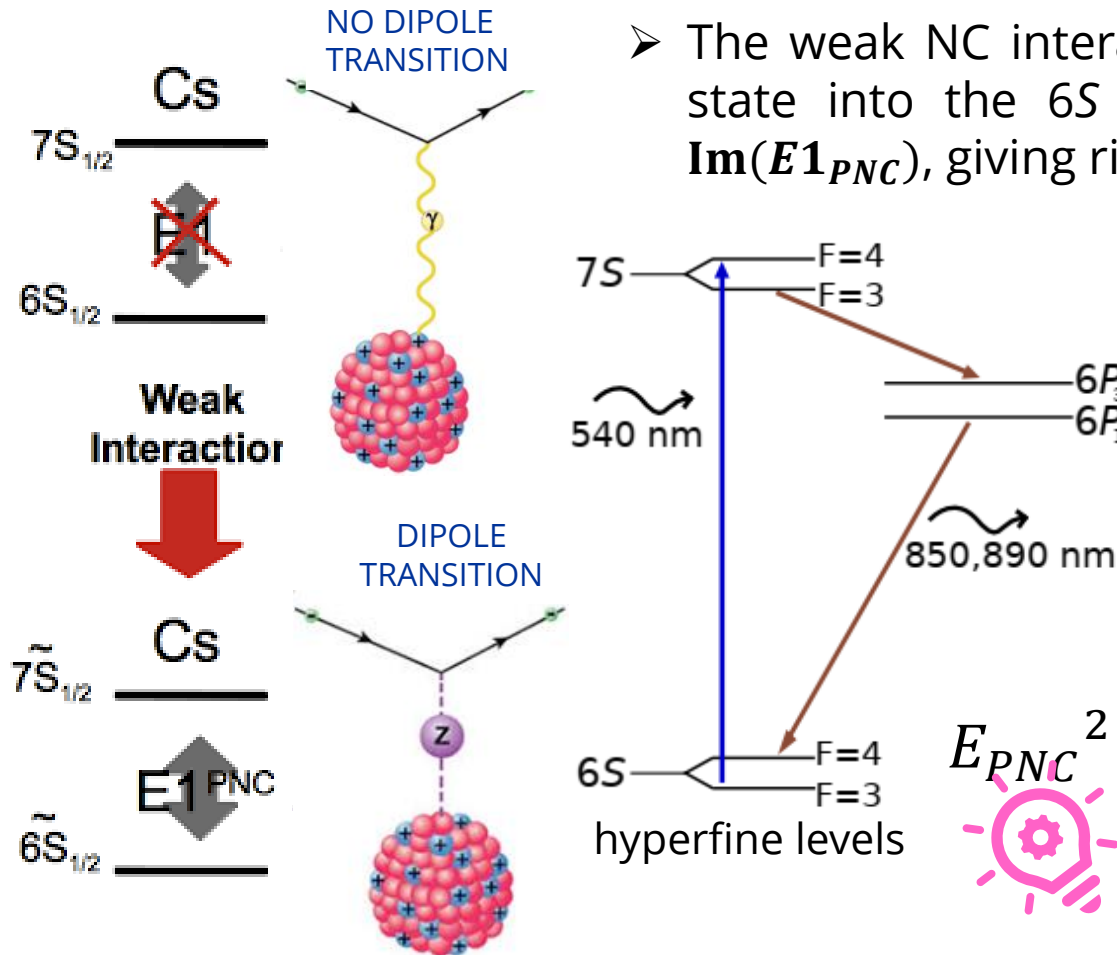
+ COHERENT + APV



Atomic parity violation* on Cs

*also known as PNC
(Parity nonconservation)

- In the absence of electric fields and weak neutral currents, **an electric dipole** (E1) transition between two **atomic states with same parity** (6S and 7S in Cs) is forbidden by the parity selection rule.
- However an **electric dipole transition amplitude** can be induced by a Z boson exchange between atomic electrons and nucleons → Atomic Parity Violation (APV)



➤ The weak NC interaction violates parity and mixes a small amount of the *P* state into the 6S and 7S states ($\sim 10^{-11}$), characterized by the quantity $\text{Im}(\mathbf{E1}_{PNC})$, giving rise to a **7S → 6S transition**.

➤ To obtain an observable that is at first order in this amplitude, an electric field **E** (that also mixes S & P) is applied. **E** gives rise to a “**Stark induced**” E1 transition amplitude, A_E that is typically 10^5 times larger than A_{PNC} and can **interfere** with it.

$$R_{7S \rightarrow 6S} = |A_E \pm A_{PNC}|^2 = E1_\beta^2 \pm 2E1_\beta \mathbf{E1}_{PNC} +$$

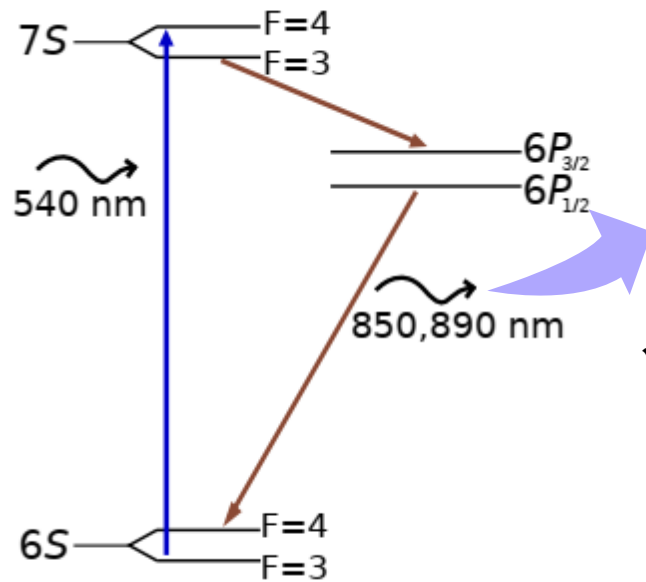
Because the interference term is linear in $\mathbf{E1}_{PNC}$ it can be large enough to be measured, but it must be distinguished from the large background contribution ($E1_\beta^2$).

The experimental technique

For there to be a nonzero interference term, **the experiment must have a “handedness”**, and if the handedness is reversed, the [interference term will change sign](#), and can thereby be distinguished as a modulation in the transition rate

$$R_{7S \rightarrow 6S} = |A_E \pm A_{PNC}|^2 \simeq E1_\beta^2 \pm 2E1_\beta E1_{PNC}$$

- **Stark-interference technique:** cesium atoms pass through a region of perpendicular electric, magnetic, and laser fields. **The “handedness” of the experiment is changed by reversing the direction of all fields.**



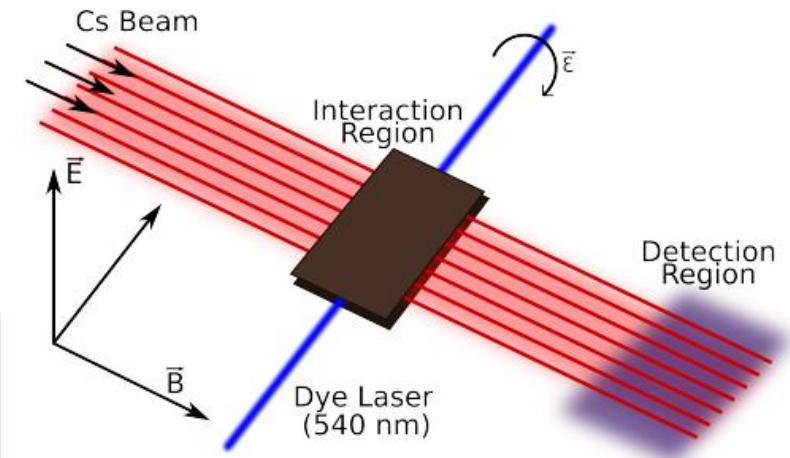
The transition rate is obtained by measuring the amount of 850- and 890-nm light emitted in the 6P-6S step of the 7S-6S decay sequence.

- ✓ The measurements culminated in 1997 when the Boulder group performed a measurement of A_{PNC}/A_E with an uncertainty of just 0.35%.

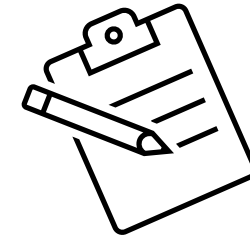
$$\text{Im} \left(\frac{E_{PNC}}{\beta} \right) = -1.5935(56) \frac{\text{mV}}{\text{cm}}$$

[C. S. Wood et al., Science **275**, 1759 (1997)]

The PV amplitude is in units of the equivalent electric field required to give the same mixing of *S* and *P* states as the PV interaction



Extracting the weak charge from APV



$$Q_W = N \left(\frac{\text{Im } E_{\text{PNC}}}{\beta} \right)_{\text{exp.}} \left(\frac{Q_W}{N \text{Im } E_{\text{PNC}}} \right)_{\text{th.}} \beta_{\text{exp.}+\text{th.}}$$

+ Experimental value of **electric dipole transition amplitude** between 6S and 7S states in Cs

[=] C. S. Wood et al., Science **275**, 1759 (1997)

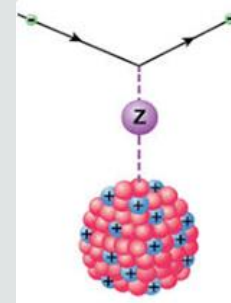
[=] J. Guena, et al., PRA **71**, 042108 (2005)

PDG2020 average

$$\text{Im} \left(\frac{E_{\text{PNC}}}{\beta} \right) = -1.5924(55) \text{ mV/cm}$$

✓ Theoretical amplitude of the electric dipole transition

$$E_{\text{PNC}} = \sum_n \left[\frac{\langle 6s | H_{\text{PNC}} | np_{1/2} \rangle \langle np_{1/2} | \mathbf{d} | 7s \rangle}{E_{6s} - E_{np_{1/2}}} + \frac{\langle 6s | \mathbf{d} | np_{1/2} \rangle \langle np_{1/2} | H_{\text{PNC}} | 7s \rangle}{E_{7s} - E_{np_{1/2}}} \right],$$



➤ where \mathbf{d} is the electric dipole operator, and

$$H_{\text{PNC}} = -\frac{G_F}{2\sqrt{2}} Q_W \gamma_5 \rho(\mathbf{r})$$

Value of $\text{Im} E_{\text{PNC}}$ used by PDG (V. Dzuba *et al.*, PRL **109**, 203003 (2012))

$$\text{Im } E_{\text{PNC}} = (0.8977 \pm 0.0040) \times 10^{-11} |e| a_B Q_W / N$$

nuclear Hamiltonian describing the **electron-nucleus weak interaction**

$\rho(\mathbf{r}) = \rho_p(\mathbf{r}) = \rho_n(\mathbf{r}) \rightarrow$ **neutron skin correction** needed

see also



β : tensor transition polarizability

It characterizes the size of the Stark mixing induced electric dipole amplitude (external electric field)



[=] Bennet & Wieman, PRL **82**, 2484 (1999)
Dzuba & Flambaum, PRA **62** 052101 (2000)

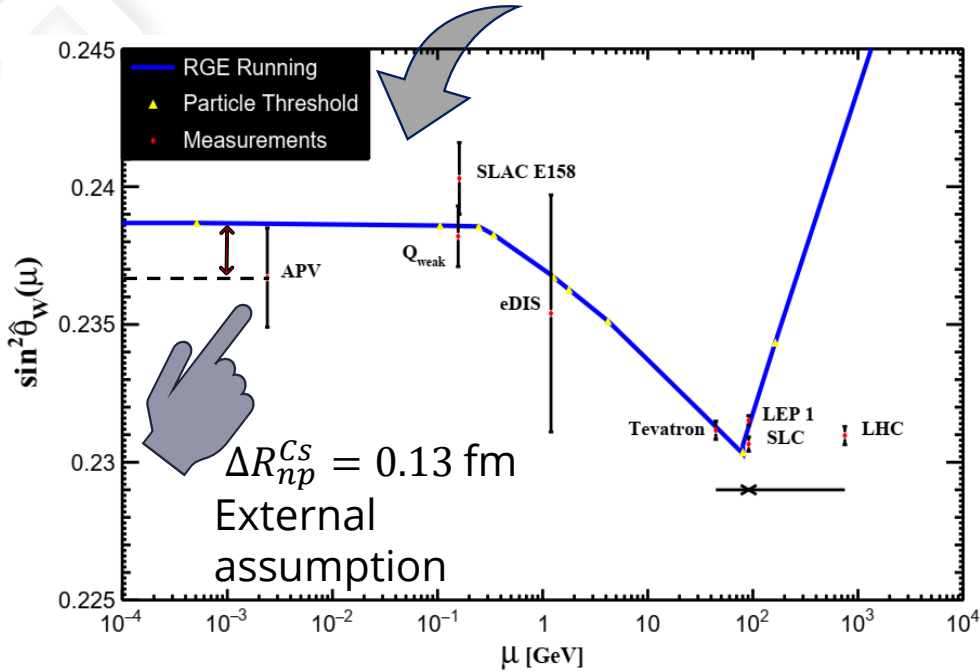
PDG2020 average
 $\beta = 27.064(33) a_B^3$

NEW result on $\text{Im} E_{\text{PNC}}$!

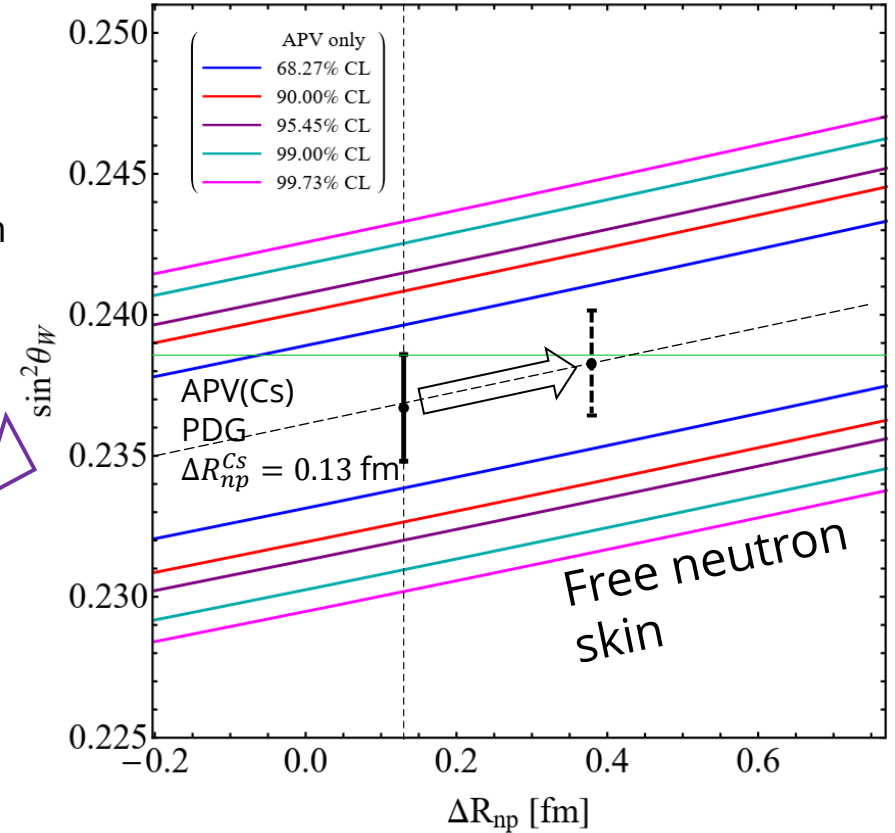
➤ I will refer with **APV2021** when using $\text{Im } E_{\text{PNC}}$ from B. K. Sahoo et al. PRD **103**, L111303 (2021)

Weak mixing angle from APV(Cs)

Historically APV(Cs) has been used to extract the **lowest energy determination of the weak mixing angle**.



However R_n (Cs) (or the neutron skin) has been taken from **indirect measurements** using antiprotonic atoms, which are known to be affected by considerable model dependencies



+ In order to measure R_n one has to subtract to the so-called “neutron skin” correction in order to obtain

$$\delta E_{\text{PNC}}^{\text{n.s.}}(R_n) = [(N/Q_W) (1 - (q_n(R_n)/q_p)) E_{\text{PNC}}^{\text{w.n.s.}}]$$

$$q_{p,n} = 4\pi \int_0^\infty \rho_{p,n}(r) f(r) r^2 dr \quad \text{Where } \mathbf{p(r)} \text{ are the proton and neutron densities in the nucleus.}$$

✓ The theoretical PNC amplitude of the electric dipole transition is calculated from atomic theory to be

$$\text{Im } E_{\text{PNC}} = (0.8977 \pm 0.0040) \times 10^{-11} |e| a_B Q_W / N$$

Value of $\text{Im } E_{\text{PNC}}$ used by PDG (V. Dzuba *et al.*, PRL 109, 203003 (2012))
I will refer to it with “APV PDG”.

But, we also use



NEW result on $\text{Im } E_{\text{PNC}}$!

➤ I will refer with **APV 2021** when usign $\text{Im } E_{\text{PNC}}$ from B. K. Sahoo *et al.* PRD 103, L111303 (2021)

Atomic Parity Violation for weak mixing angle measurements

✓ Weak charge in the SM including radiative corrections

Using SM prediction at low energy
 $\sin^2 \hat{\theta}_W(0) = 0.23857(5)$

$$Q_W^{SM+r.c.} \equiv -2[Z(g_{AV}^{ep} + 0.00005) + N(g_{AV}^{en} + 0.00006)] \left(1 - \frac{\alpha}{2\pi}\right) \approx Z(1 - 4 \sin^2 \theta_W^{SM}) - N$$



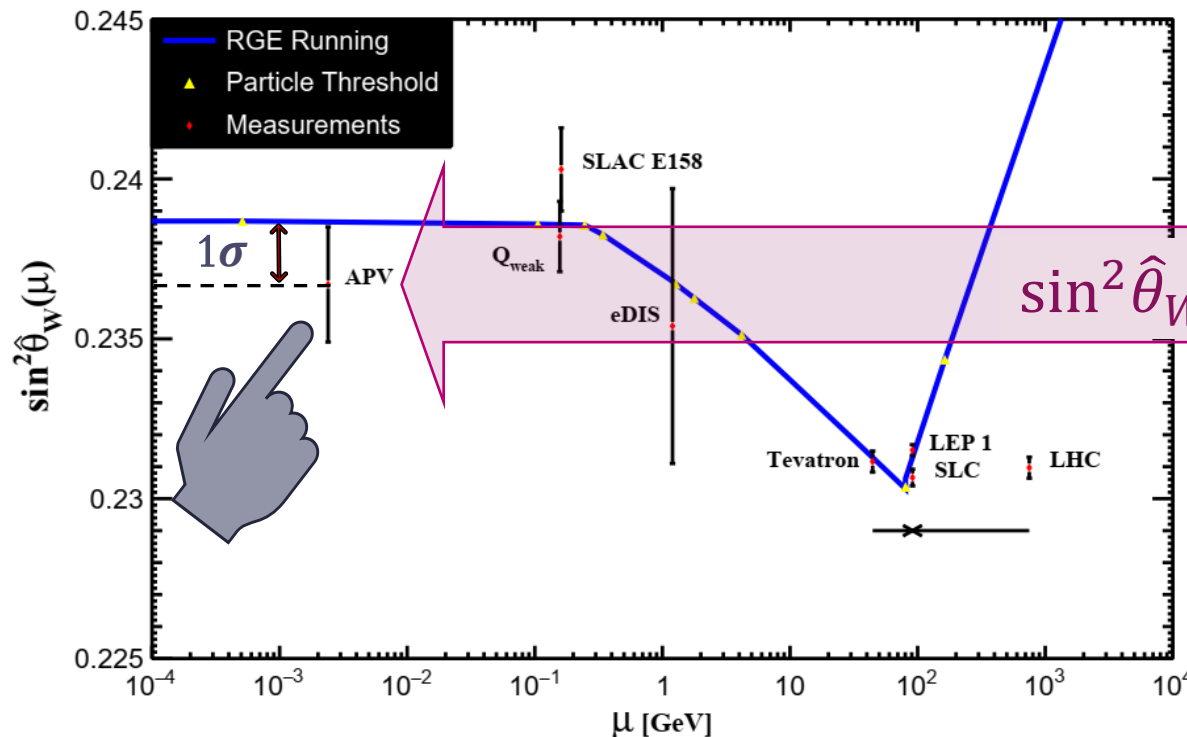
Theoretically

$$Q_W^{SM\text{ th}}(^{133}_{55}\text{Cs}) = -73.23(1)$$

1σ difference

Experimentally

$$Q_W^{\text{exp.}}(^{133}_{55}\text{Cs}) = -72.82(42)$$



$$\sin^2 \hat{\theta}_W(2.4 \text{ MeV}) = 0.2367 \pm 0.0018$$

But which Cs neutron skin correction is used?

The dilemma



APV (Cs)

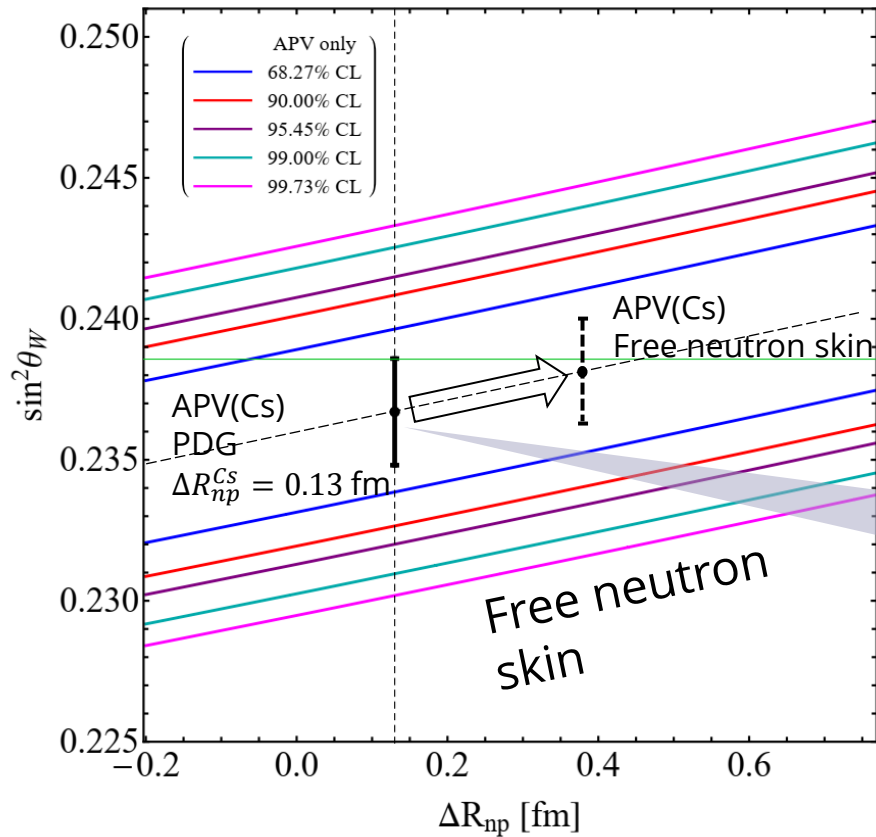
- + Sensitive to the weak mixing angle
- + Similarly sensitive to the neutron skin

COHERENT (CsI)

- + CE ν NS is sensitive to the neutron skin
- + But less sensitive to the weak mixing angle

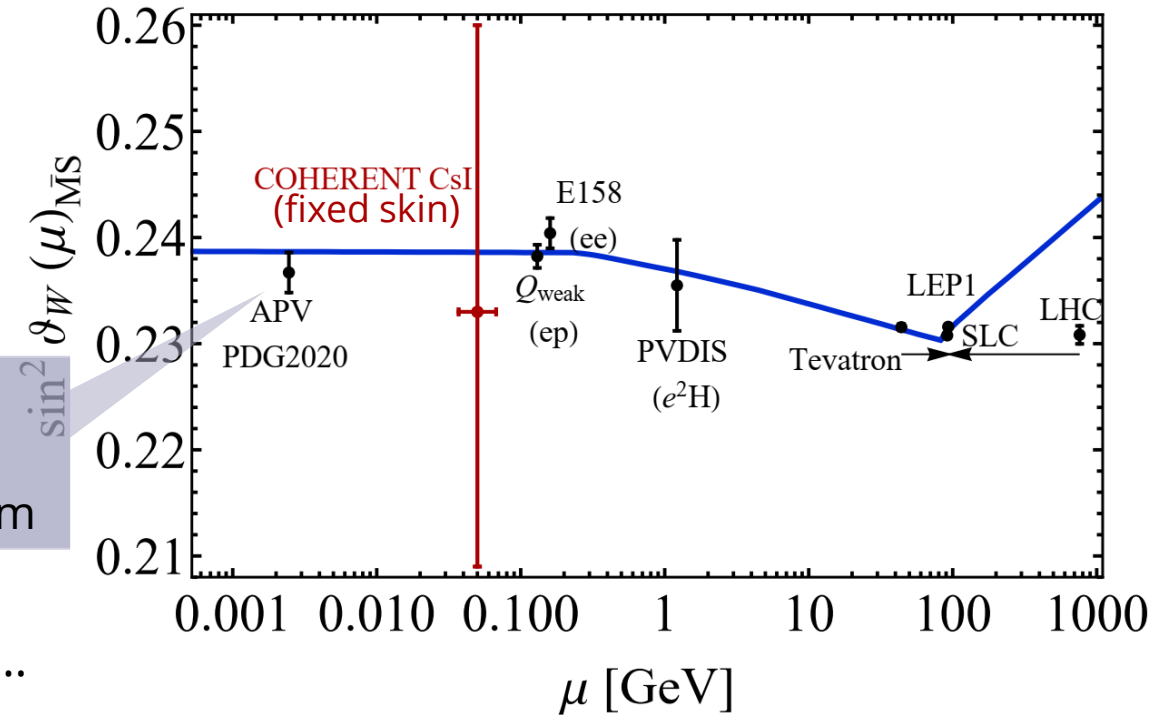


$$\sin^2 \vartheta_W(\text{COH} - \text{CsI}) = 0.231^{+0.027}_{-0.024}(1\sigma)^{+0.046}_{-0.039}(90\% \text{CL})^{+0.058}_{-0.047}(2\sigma)$$

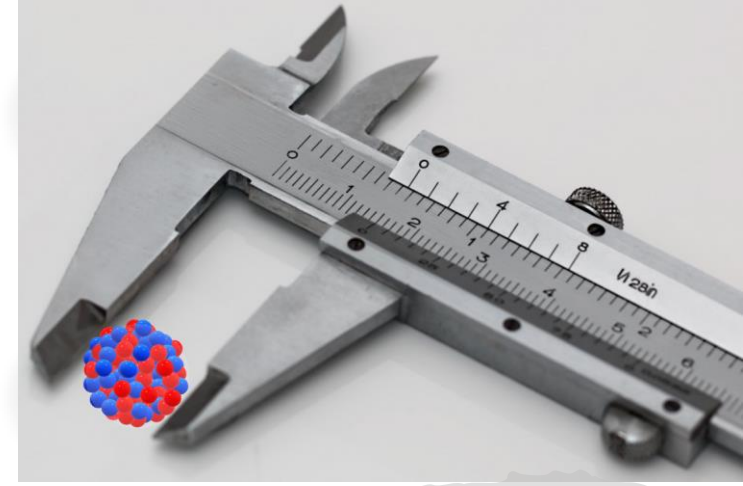


APV(Cs) PDG
corresponds to
 $\Delta R_{np}^{Cs}(\text{Extr.}) = 0.13 \text{ fm}$

Extrapolated from
antiprotonic atoms...

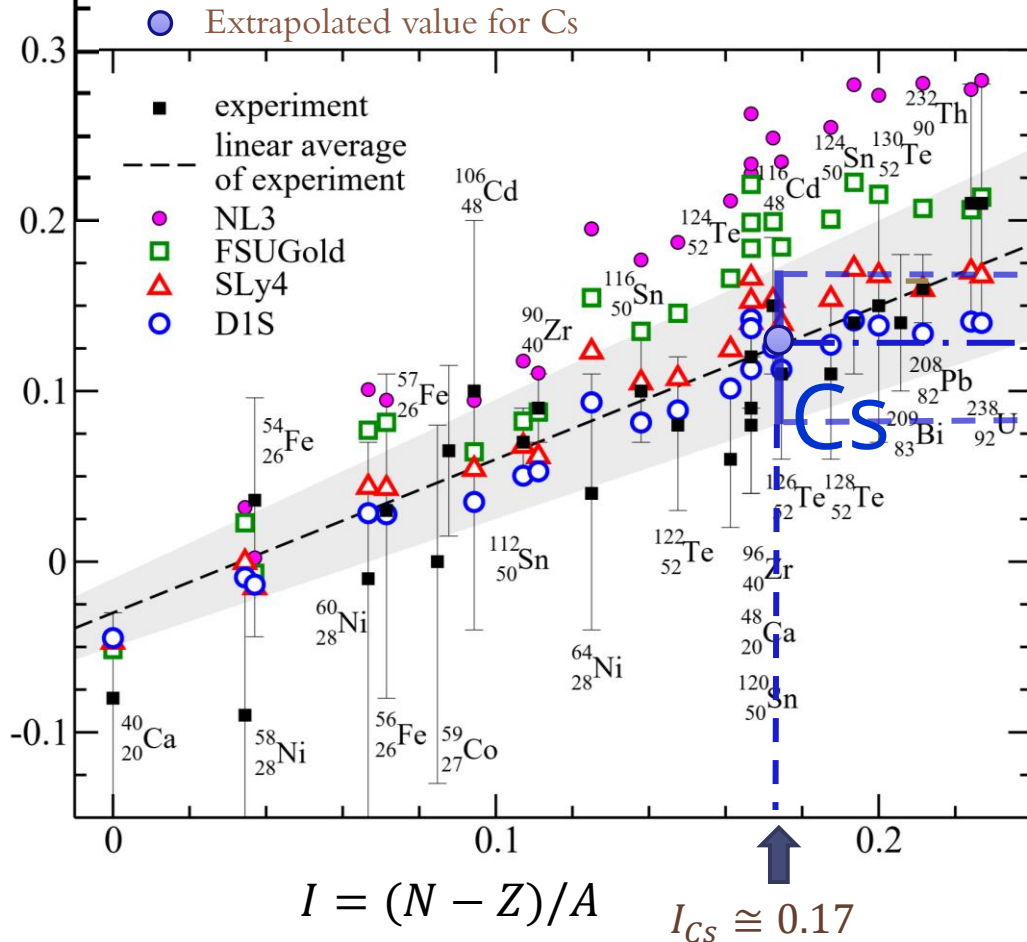


Extrapolated value of ΔR_{np}^{Cs}



+ Neutron-skin of a variety of nuclei as extracted from **antiprotonic data** as a function of the asymmetry parameter, I .

✓ From this **linear fit** one obtains the relation for the neutron skin for every nuclei



$$\Delta R_{np}[\text{fm}] = -(0.04 \pm 0.03) + (1.01 \pm 0.15) \frac{N - Z}{A}$$

For cesium it gives

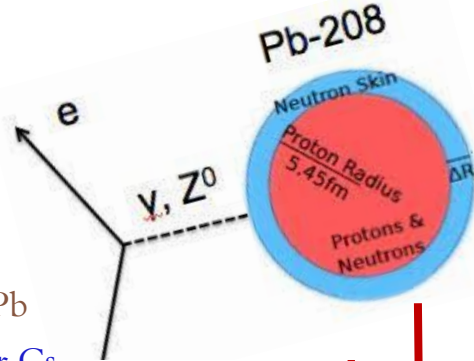
$$\Delta R_{np}^{Cs}(\text{extrap}) \cong 0.13 \pm 0.04 \text{ fm}$$

Extrapolated (not measured) value for cesium!

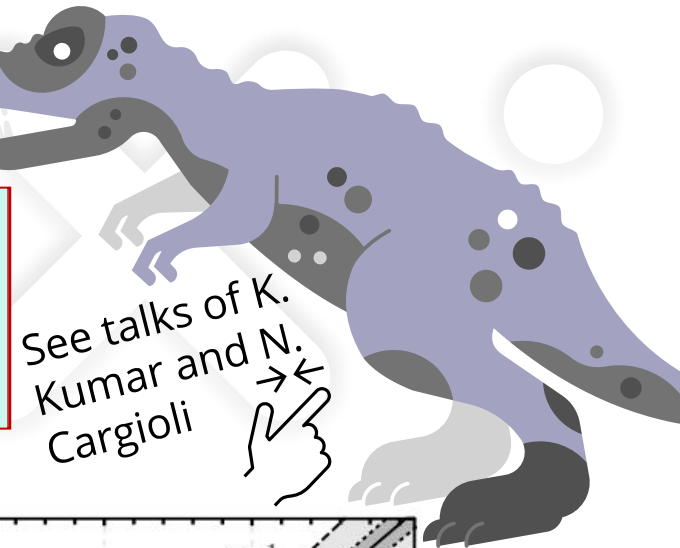


Antiprotonic data: radiochemical and the other based on x-ray data constraining the **neutron distribution at the nuclear periphery**

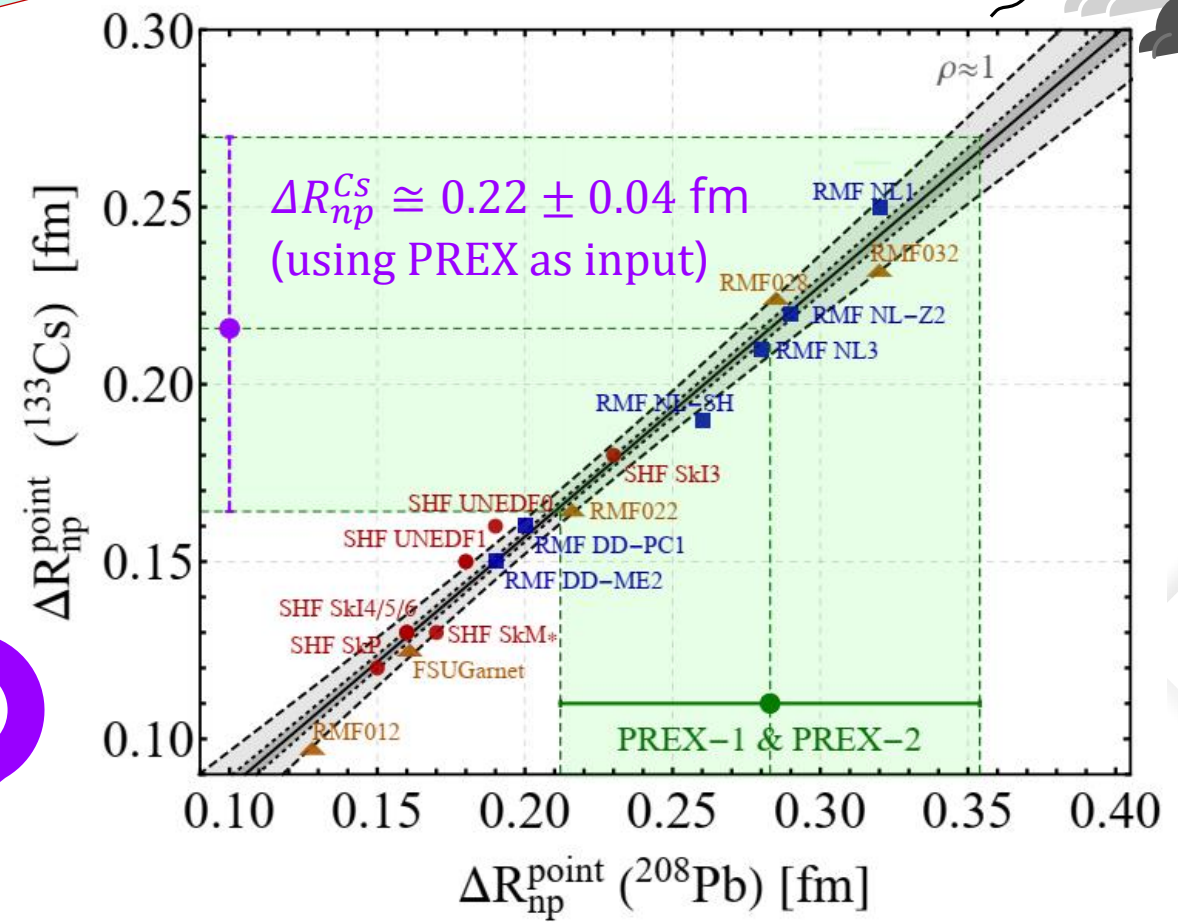
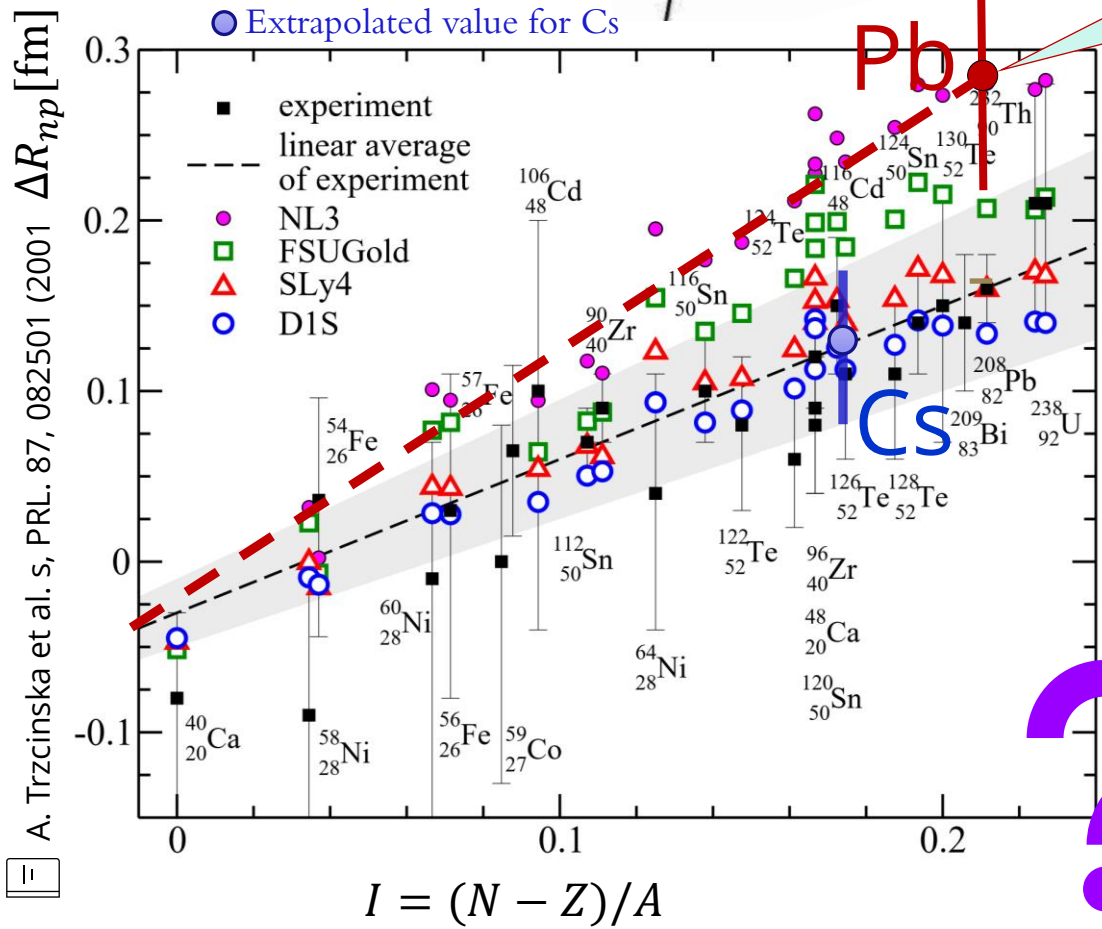
Extrapolated value of ΔR_{np}^{Cs}



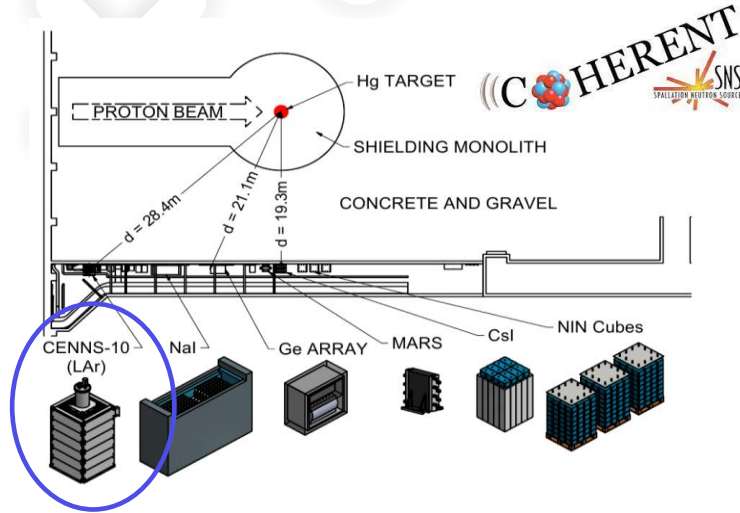
PREX-I & PREX-II
 $\Delta R_{np}^{Pb} = 0.283 \pm 0.071 \text{ fm}$
 D. Adhikari et al. PRL 126, 172502 (2021)



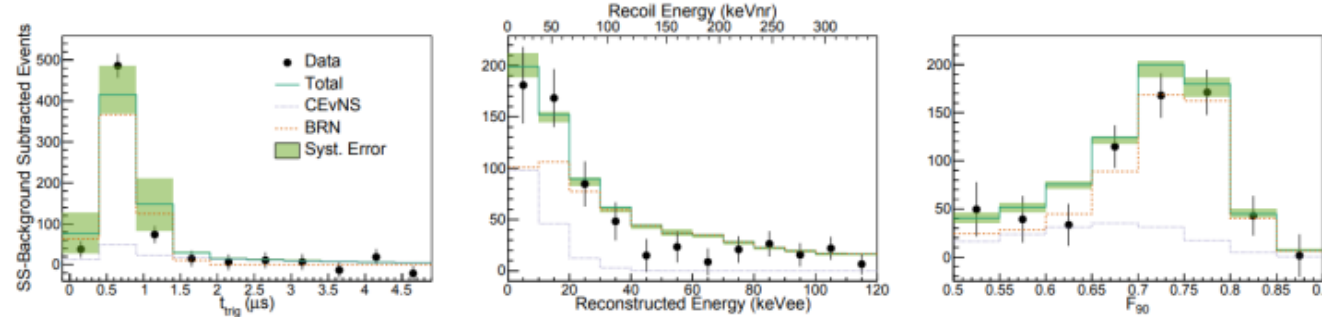
See talks of K. Kumar and N. Cargioli



Neutron nuclear radius in argon

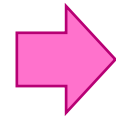


Combined fit in (time, energy, PSP) space suggest $>3\sigma$ CEvNS detection significance



Dominant backgrounds:
1. ^{39}Ar beta decay
2. Beam related neutrons

— Akimov et al, COHERENT Coll. PRL 126, 01002 (2021)



COHERENT Argon

$$R_n(^{40}\text{Ar}) < 4.2 \text{ fm}$$

More statistics needed.

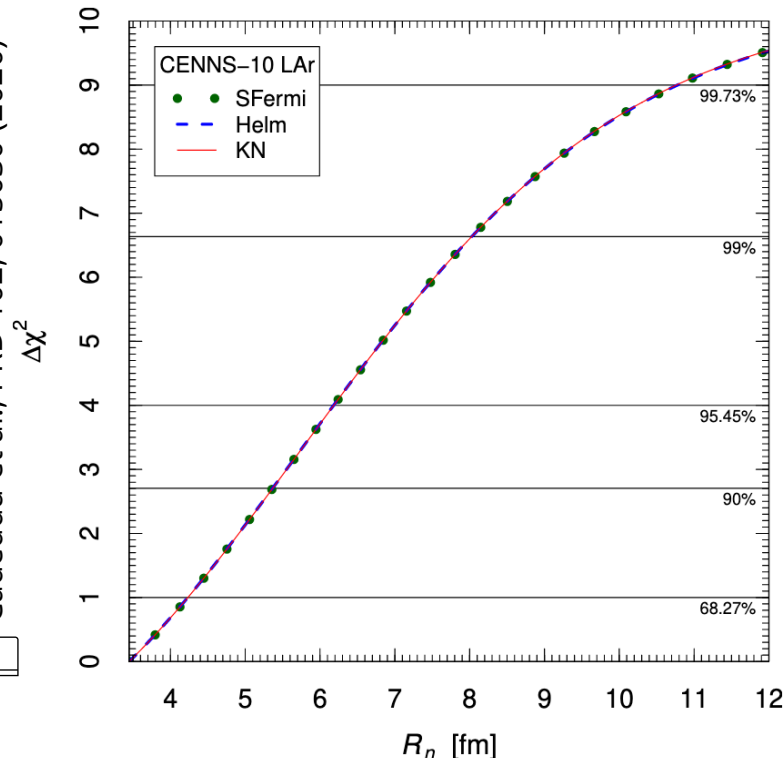
Theoretical values

Interaction	R_p^{point}	R_n^{point}
Sky3D		
SkI3	3.33	3.43
SkI4	3.31	3.41
Sly4	3.38	3.46
Sly5	3.37	3.45
Sly6	3.36	3.44
Sly4d	3.35	3.44
SV-bas	3.33	3.42
UNEDF0	3.37	3.47
UNEDF1	3.33	3.43
SkM*	3.37	3.45
SkP	3.40	3.48

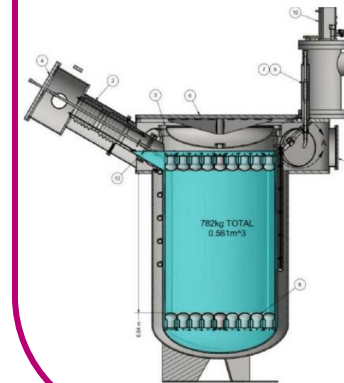
— See also:
Payne et al.,
PRC 100, 061304 (2019)

— See also:
Miranda et al.,
JHEP 05 (2020) 130

— Cadeddu et al., PRD 102, 015030 (2020)

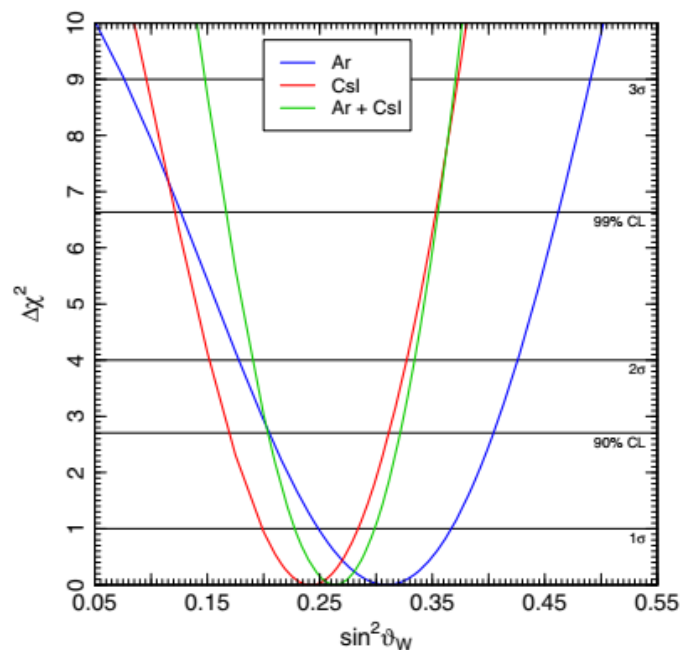
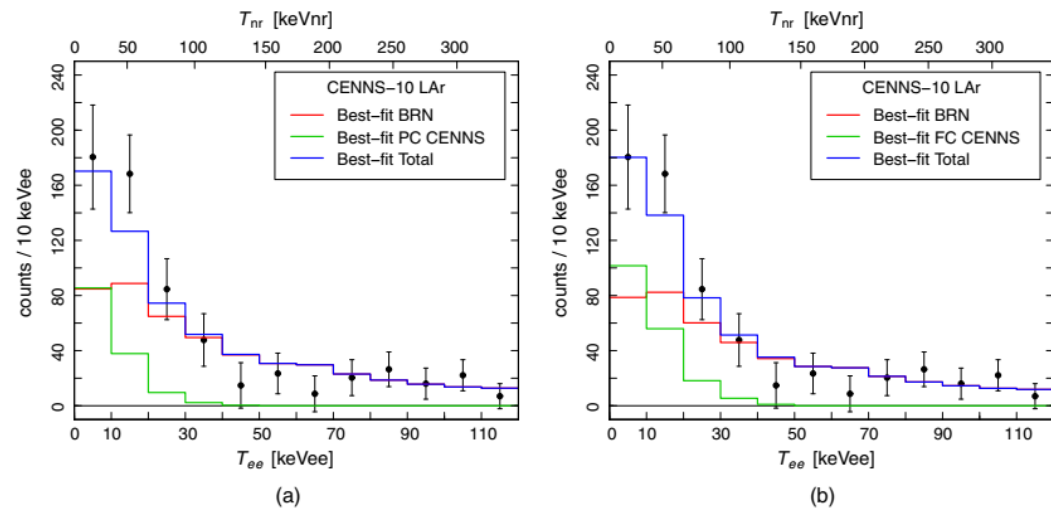


COHERENT future argon: "COH-Ar-750"
LAr based detector for precision CEvNS



- Single phase, scintillation only, 750 kg total (610 kg fiducial)
- 3000 CEvNS/year

$$\chi^2_S = \sum_{i=1}^{12} \left(\frac{N_i^{\text{exp}} - \eta_{\text{CElNS}} N_i^{\text{CElNS}} - \eta_{\text{PBRN}} B_i^{\text{PBRN}} - \eta_{\text{LBRN}} B_i^{\text{LBRN}}}{\sigma_i} \right)^2 + \left(\frac{\eta_{\text{CElNS}} - 1}{\sigma_{\text{CElNS}}} \right)^2 + \left(\frac{\eta_{\text{PBRN}} - 1}{\sigma_{\text{PBRN}}} \right)^2 + \left(\frac{\eta_{\text{LBRN}} - 1}{\sigma_{\text{LBRN}}} \right)^2,$$



Physics results from the first COHERENT observation of coherent elastic neutrino-nucleus scattering in argon and their combination with cesium-iodide data

M. Cadeddu^{1,*}, F. Dordei^{1,†}, C. Giunti^{2,‡}, Y. F. Li^{3,4,§}, E. Picciau^{5,6,||} and Y. Y. Zhang^{3,4,¶}

¹*Istituto Nazionale di Fisica Nucleare (INFN), Sezione di Cagliari,*

Complesso Universitario di Monserrato—S.P. per Sestu Km 0.700, 09042 Monserrato (Cagliari), Italy

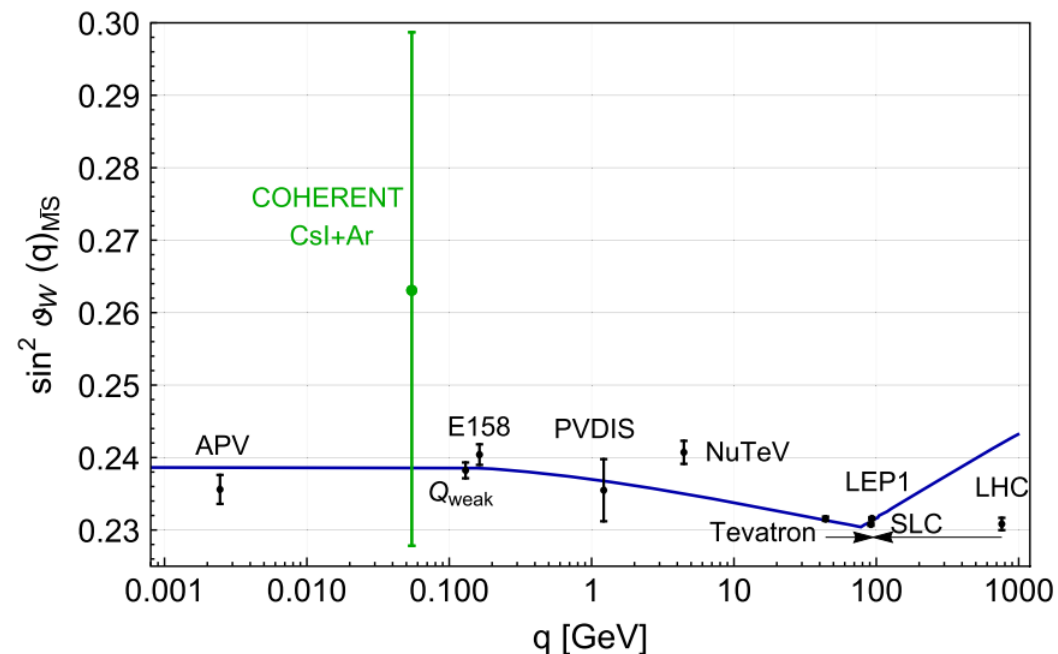
²*Istituto Nazionale di Fisica Nucleare (INFN), Sezione di Torino, Via P. Giuria 1, I-10125 Torino, Italy*

³*Institute of High Energy Physics, Chinese Academy of Sciences, Beijing 100049, China*

⁴*School of Physical Sciences, University of Chinese Academy of Sciences, Beijing 100049, China*

⁵*Dipartimento di Fisica, Università degli Studi di Cagliari, and INFN, Sezione di Cagliari, Complesso Universitario di Monserrato—S.P. per Sestu Km 0.700, 09042 Monserrato (Cagliari), Italy*

⁶*University of Massachusetts, Amherst, Massachusetts 01003, USA*



FITTING THE COHERENT CsI DATA FOR THE NEUTRON RADIUS

□ G. Fricke et al., Atom. Data Nucl. Data Tabl. 60, 177 (1995)

✓ From muonic X-rays
data we have
(For fixed $t = 2.3$ fm)

$$R_{ch}^{Cs} = 4.804 \text{ fm} \quad (\text{Cesium charge rms radius})$$

$$R_{ch}^I = 4.749 \text{ fm} \quad (\text{Iodine charge rms radius})$$

↓

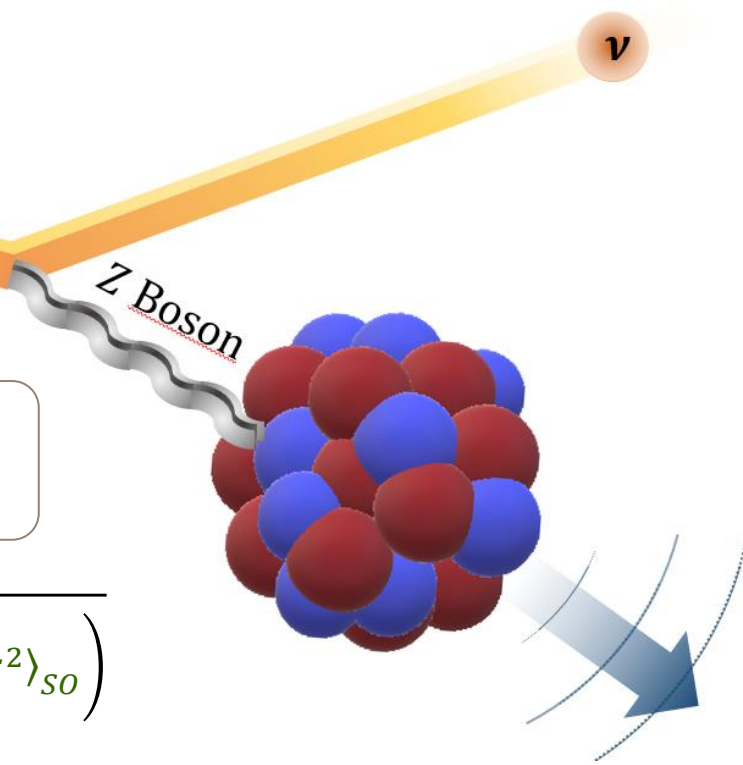
$$R_p^{\text{rms}} = \sqrt{R_{ch}^2 - \left(\frac{N}{Z} \langle r_n^2 \rangle + \frac{3}{4M^2} + \langle r^2 \rangle_{so} \right)}$$

$$R_p^{Cs} = 4.821 \pm 0.005 \text{ fm} \quad (\text{Cesium rms proton radius})$$

$$R_p^I = 4.766 \pm 0.008 \text{ fm} \quad (\text{Iodine rms-proton radius})$$

$$\frac{d\sigma}{dE_r} \cong \frac{G_F^2 m_N}{4\pi} \left(1 - \frac{m_N E_r}{2E_\nu^2} \right) \left[g_V^p Z F_Z \left(E_r, R_p^{Cs/I} \right) + g_V^n N F_N(E_r, R_n^{CsI}) \right]^2$$

R_n^{Cs} & R_n^I very well known so we fitted
COHERENT CsI data looking for R_n^{CsI} ...



FROM THE CHARGE TO THE PROTON RADIUS

One need to take into account finite size of both protons and neutrons plus other corrections



$$R_{ch}^2 = R_{point}^2 + \langle r_p^2 \rangle + \frac{N}{Z} \langle r_n^2 \rangle + \frac{3}{4M^2} + \langle r^2 \rangle_{so}$$

Charge radius

Point-proton radius

Mean squared charge radius of a single proton

$$\langle r_p^2 \rangle = 0.7071 \text{ fm}^2$$

Mean squared charge radius of a single neutron

$$\langle r_n^2 \rangle = -0.1161 \text{ fm}^2$$

[=] G. Hagen et al. *Nature Physics* 12, 186–190 (2016), Arxiv: 1509.07169

M. Cadeddu et al. PRD 102, 015030 (2020), Arxiv: 2005.01645

Relativistic Darwin-Foldy correction
~0.033 fm²

Spin-orbit correction
~0.09 fm² for ⁴⁸Ca
~0.028 fm² for ²⁰⁸Pb

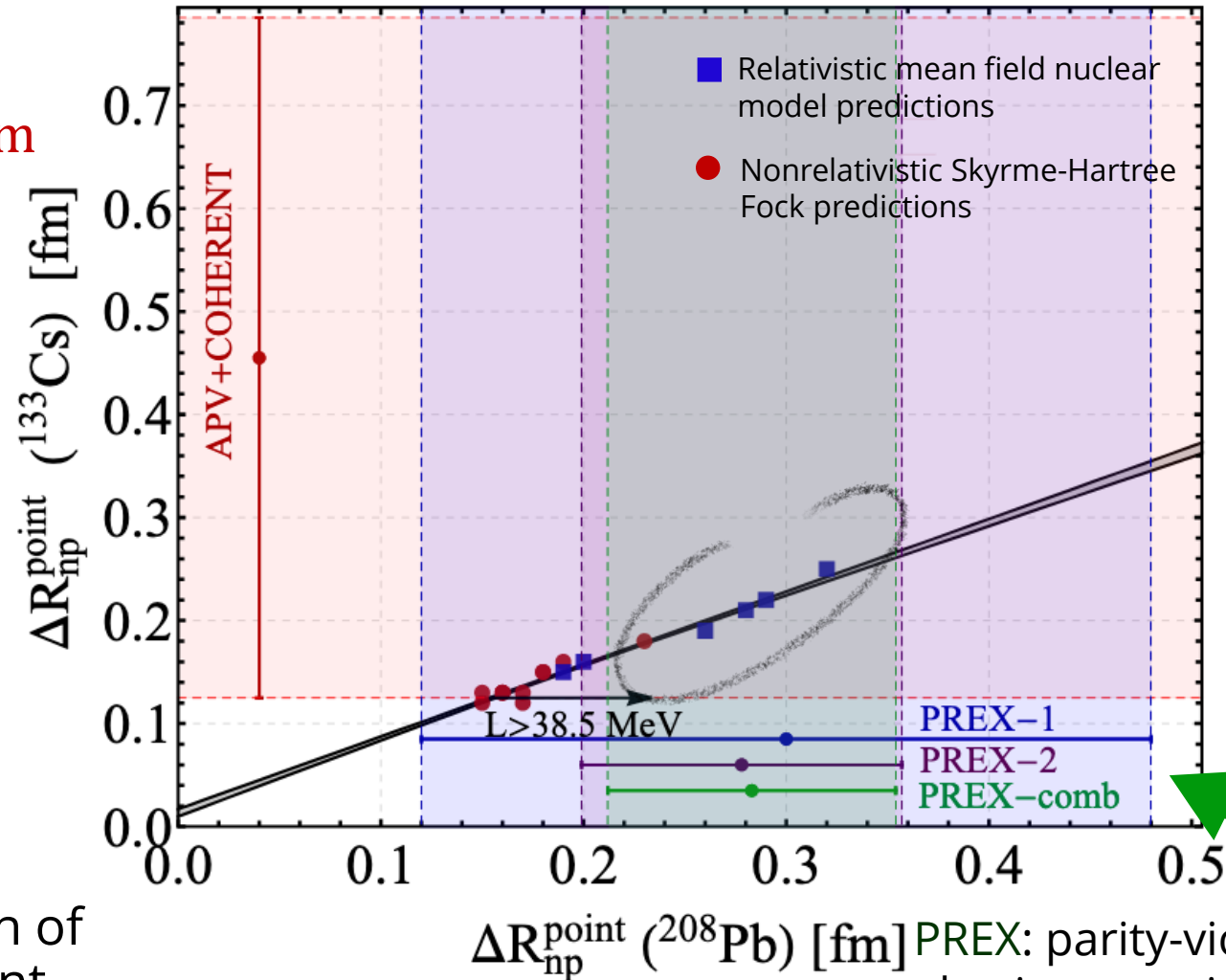
RMS proton distribution radius

$$R_p^{rms} = \sqrt{R_{point}^2 + \langle r_p^2 \rangle} = \sqrt{R_{ch}^2 - \left(\frac{N}{Z} \langle r_n^2 \rangle + \frac{3}{4M^2} + \langle r^2 \rangle_{so} \right)}$$

COHERENT+APV compared to PREX

$$\Delta R_{np}(^{133}\text{Cs}) = 0.45^{+0.33}_{-0.33} \text{ fm}$$

@fixed $\sin^2 \hat{\theta}_w$



Cadeddu et al., PRC 104, 065502
arXiv:2102.06153

+ Strong linear correlation between the neutron skin of Cs and Pb among different nuclear model predictions

PREX, PRL 126, 172502 (2021)

$$A_{\text{PV}} = \frac{\sigma_R - \sigma_L}{\sigma_R + \sigma_L} \approx \frac{G_F Q^2 |Q_W|}{4\sqrt{2}\pi\alpha Z} \frac{F_W(Q^2)}{F_{\text{ch}}(Q^2)}$$

PREX: parity-violating asymmetry in the elastic scattering of longitudinally polarized electrons on ^{208}Pb

The proton form factor

$$\frac{d\sigma_{\nu-CsI}}{dT} = \frac{G_F^2 M}{4\pi} \left(1 - \frac{MT}{2E_\nu^2}\right) [N \mathbf{F}_N(T, R_n) - \varepsilon Z \mathbf{F}_Z(T, R_p)]^2$$



The proton structures of $^{133}_{55}\text{Cs}$ ($N = 78$) and $^{127}_{53}\text{I}$ ($N = 74$) have been studied with muonic spectroscopy and the data were fitted with **two-parameter Fermi density distributions** of the form

$$\rho_F(r) = \frac{\rho_0}{1 + e^{(r-c)/a}}$$

Where, the **half-density radius** c is related to the **rms radius** and the a parameter quantifies the **surface thickness** $t = 4a \ln 3$ (in the analysis fixed to 2.30 fm).

- Fitting the data they obtained

$$R_{ch}^{Cs} = 4.804 \text{ fm} \quad (\text{Caesium proton rms radius})$$

$$R_{ch}^I = 4.749 \text{ fm} \quad (\text{Iodine proton rms radius})$$

